

# Surface-ionization field mass-spectrometry studies of nonequilibrium surface ionization

N M Blashenkov, G Ya Lavrent'ev

DOI: 10.1070/PU2007v050n01ABEH006115

## Contents

<b>1. Introduction</b>	<b>53</b>
<b>2. Surface ionization in nonequilibrium systems. General ideas</b>	<b>54</b>
2.1 Surface ionization in nonequilibrium and highly nonequilibrium systems; 2.2 Dissociative surface ionization of polyatomic molecules; 2.3 The kinetics of monomolecular reactions on a surface; 2.4 Surface ionization of products of the monomolecular heterogeneous disintegration of molecules; 2.5 Surface ionization in the monomolecular disintegration of fragments of a multimolecular complex; 2.6 The formation kinetics of fragments of a multimolecular complex	
<b>3. Nonequilibrium surface ionization. General ideas</b>	<b>58</b>
3.1 Statistical derivation of the degree of nonequilibrium surface ionization; 3.2 Statistical derivation of the degree of nonequilibrium surface ionization in an electric field; 3.3 Nonequilibrium surface ionization of fragments of multimolecular complexes	
<b>4. Method</b>	<b>60</b>
4.1 Surface-ionization field mass spectrometry; 4.2 The shape of the temperature dependences of the ion current as a function of the electric field strength; 4.3 The lifetime and the energy distribution function of ions as functions of the electric field strength; 4.4 The possibility of determining the shape of potential curves characterizing the interaction of polyatomic ions with a surface; 4.5 Photodesorption field IR spectroscopy; 4.6 The possibility of estimating the absorption of IR radiation by adsorbed molecules	
<b>5. Experiments and a discussion</b>	<b>65</b>
5.1 Determining the parameters of dissociative surface ionization of polyatomic molecules; 5.2 Relaxation of the energy distribution functions of products of dissociative surface ionization; 5.3 Magnitude of departure from equilibrium in endothermic reactions on a surface; 5.4 Times of energy exchange between reaction products and the surface; 5.5 Interaction potentials between polyatomic ions and the surface; 5.6 A physically adsorbed state of polyatomic ions near a metal surface in an electric field accelerating ions; 5.7 Determining the parameters of surface multimolecular complexes; 5.8 Ionization of energy-saturated compounds on a surface — nonequilibrium surface ionization; 5.9 Optical radiation and the ionization of hydrogen atoms under nonequilibrium surface ionization in an electric field; 5.10 Nonequilibrium surface ionization with external excitation of the vibrational states of the adsorbate (photodesorption field IR spectroscopy); 5.11 Absorption cross section of IR radiation by adsorbed molecules; 5.12 Ratio of partition functions of the neutral and ionic states in a polyatomic molecule	
<b>6. Conclusions</b>	<b>77</b>
<b>References</b>	<b>77</b>

**Abstract.** The ionization of polyatomic molecules on tungsten and tungsten oxide surfaces is considered for quasiequilibrium or essentially nonequilibrium conditions (in the latter case, the term nonequilibrium surface ionization is used for adsorbate ionization). Heterogeneous reactions are supposed to proceed through monomolecular decay of polyatomic molecules or fragments of multimolecular complexes. The nonequilibrium nature

of these reactions is established. The dependences of the current density of disordered ions on the surface temperature, electric field strength, and ionized particle energy distribution are obtained in analytical form. Heterogeneous dissociation energies, the ionization potentials of radicals, and the magnitude of reaction departure from equilibrium are determined from experimental data, as are energy exchange times between reaction products and surfaces, the number of molecules in molecular complexes, and the number of effective degrees of freedom in molecules and complexes. In collecting the data a new technique relying on surface-ionization field mass spectrometry was applied.

N M Blashenkov, G Ya Lavrent'ev A F Ioffe Physico-Technical Institute, Russian Academy of Sciences, ul. Politekhnikeskaya 26, 194021 St.-Petersburg, Russian Federation Tel. (7-812) 292 89 14, 292 89 48. Fax (7-812) 297 10 17 E-mail: N.Blashenkov@mail.ioffe.ru, jakov67@mail.ru

Received 2 May 2006, revised 10 July 2006  
Uspekhi Fizicheskikh Nauk 177 (1) 59–85 (2007)  
Translated by E Yankovsky; edited by A Radzig

## 1. Introduction

The theory of surface ionization [1] describes the formation of ions in the process of thermal desorption of atoms and molecules from the surface of a conducting solid. The

temperature of the Boltzmann energy distribution of all the particles being desorbed is equal to the surface temperature.

The quantitative characteristic of surface ionization is the degree  $\alpha$  of surface ionization, equal to the ratio of the fluxes  $g_+$  and  $g_0$  of the ions and atoms undergoing desorption which depends on the ionization potential  $eV$  of the atoms, the work function  $e\phi$ , the surface temperature  $T$ , and the ratio  $A$  of the statistical weights of the ionic and atomic states (the Saha – Langmuir formula). The effect of an electric field  $F$  on surface ionization is described by what is known as the extended Saha – Langmuir formula [2]

$$\alpha = \frac{g_+}{g_0} = A \exp \left[ \frac{e(\phi - V + \sqrt{eF})}{k_B T} \right].$$

The relation between the experimental value of thermal ion current  $j$  and the flux density  $g$  of atoms adsorbable on the surface of the emitter can be expressed in terms of the surface-ionization coefficient  $\beta = g_+/g$  as follows:

$$j = eg_+ = eg\beta = \frac{eg}{1 + 1/\alpha},$$

since in the steady-state regime  $g = g_0 + g_+$ .

In the 1960s, the ideas and methods of studying the surface ionization of atoms and simple molecules were extended to polyatomic molecules [3] whose surface-ionization characteristics  $[j(T, F)]$  proved to be much more complicated. In our view, the most natural interpretation of the deviation of the function  $j(T, F)$  from the exponential as a manifestation of nonequilibrium states and processes taking place in the adsorbed layer so far has received little attention. Nevertheless, the fundamental pioneering studies of surface ionization for a large number of organic molecules [4] have clarified the phenomenological laws governing the surface ionization of polyatomic compounds, which has made it possible to predict the characteristic features of surface ionization for many classes of substances and to determine their emission constants.

Studies of the surface ionization of polyatomic compounds have revealed the formation of metastable ions that had undergone transformation and disintegration after desorption [4, 5]. To describe the transformation of polyatomic molecules into  $i$  types of new particles, the notion of  $i$  effective fluxes  $g_i$  was introduced. The total flux is related to  $g_i$  through the coefficient  $\gamma_i$  ( $g_i = \gamma_i g$ ) which determines the concentration of the  $i$ th particles that form in the adsorbed layer as a result of the processes in this layer [4]. In this representation, complex functions  $\gamma_i(T, F)$  interpreted as equilibrium dependences are actually strictly empirical. The above expressions for  $\alpha$ ,  $\beta$ , and  $j$  are also valid for surface ionization of the  $i$ th particles:  $j_i = e\gamma_i g\beta_i$ . In most cases of surface ionization of polyatomic molecules and radicals, the energy distribution of ions is an equilibrium one [4].

In addition to all this, as a result of our experiments we discovered that there can be thermally nonequilibrium ionization, for instance, when the energy liberated in the disintegration of molecules on a surface plays a significant role in the ionization of fragments [6].

Generally, the theory of nonequilibrium surface ionization describes the evaporation and ionization of polyatomic particles adsorbed on the surface of a solid, particles that reside either in vibrationally excited or vibrationally deactivated states in relation to the states determined by the surface temperature. This definition suggests that nonequilibrium

surface ionization is characterized by one more, additional, parameter, namely, the temperature  $T_n$  corresponding to the energy distribution of the adsorbed particles, which for vibrationally excited molecules is higher than the surface temperature, while for deactivated molecules it is lower. Hence, ionization of this type cannot be described by emission relationships following from the surface-ionization theory.

The 1950s saw the development of theories of monomolecular disintegration in the gas phase, theories that studied processes with nonequilibrium energy distribution functions of the products that formed in the reactions [7]. At the same time, the theory describing the kinetics of essentially nonequilibrium processes and the theory of self-organization of open systems were being actively developed.

In energy-open systems, the distribution functions (in energy, level population, etc.) are characterized not by one, as in the case of equilibrium systems, but by two or more parameters [8]. It was natural to expect that these fundamental processes should manifest themselves in the surface ionization of polyatomic molecules. For instance, energy-saturated compounds that are involved in the disintegration process can be considered as being energy-open systems, while the presence of metastable ions suggests that the polyatomic molecules at the surface accumulate considerable amounts of energy in their intramolecular bonds, which makes it possible to invoke the mechanism of monomolecular reactions described, among other things, by nonequilibrium distribution functions, for calculating the heterogeneous dissociation reactions.

In the light of all this, it came as a surprise that in the surface ionization of the majority of the polyatomic molecules that had undergone dissociation at the surface, ions with equilibrium energy distribution functions were desorbed. This can be related to the fact that polyatomic ions have on-surface lifetimes long enough for their nonequilibrium distribution functions to relax to equilibrium distribution functions before the desorption of ions begins. What this suggests is that a comprehensive study of the ionization of polyatomic particles on a surface requires experiments in which the relaxation of the distribution function of ions from the moment of their formation is investigated. The possibility of such an investigation is presented, in principle, by the method of controllable lowering of the Schottky barrier through the application of an electric field, i.e., controllable variation of the lifetime of ions at the surface, implemented in relation to the surface ionization of polyatomic molecules in our research (see Ref. [9]). Processing these data requires building a phenomenological theory that would describe both the nonequilibrium surface ionization with a calculation of the yield of the reaction products [with a derivation of the explicit form of the function  $j(T, T_n, F)$ ] and the surface ionization with nonequilibrium distribution functions.

## 2. Surface ionization in nonequilibrium systems. General ideas

### 2.1 Surface ionization in nonequilibrium and highly nonequilibrium systems

For the case of nonequilibrium systems it has proved convenient to classify the processes of disintegration and surface ionization of polyatomic particles according to the characteristic times, which are used, for instance, in the theory

of activated complexes [10]. In addition, researchers invoke the lifetimes of ions on a surface and the temperature characterizing the quasi-Maxwell–Boltzmann energy distribution (below we call this the distribution function) of the ions being formed:  $\tau_a$ , the lifetime of an activated molecule at the surface;  $\tau_r$ , the excitation relaxation time;  $\tau_i$ , the lifetime on the surface of an ion that forms from the activated molecule, and  $T_n$ , the temperature characterizing the distribution function of the forming ion, which differs from the surface temperature  $T$  by  $\Delta T$ , i.e.,  $T_n = T + \Delta T$ , with  $\Delta T$  characterizing the magnitude of the process departure from an equilibrium one.

**2.1.1 Surface ionization in quasi-equilibrium systems:**  $|\Delta T| \ll T$ . In this case, surface ionization can be described (in terms of the surface-ionization theory) by the nonequilibrium energy distribution functions of particles without introducing the additional parameter  $T_n$  [7] with the various characteristic times related as follows:

$$\tau_i \gg \tau_r \gg \tau_a. \quad (1)$$

The right-hand side in inequality (1) corresponds to a rapid disintegration of activated molecules (before the process of their relaxation begins). When the active molecules disintegrate rapidly, the rate of their disintegration is determined by the rate at which such molecules form (with an activation energy  $E$ ). This suggests that the equilibrium energy distribution of the molecules is disrupted, since in equilibrium the molecules undergoing disintegration are chiefly those whose internal energy exceeds the activation energy by an amount equal to the average energy [7]. The left-hand side in inequality (1) indicates that the nonequilibrium distribution function of the ions formed before desorption has time to relax to the equilibrium distribution function with a temperature equal to the surface temperature, i.e., ions are desorbed in equilibrium states determined by the surface temperature. However, the yield of the products of the heterogeneous reaction and the temperature dependences of the ion current will be determined by the nonequilibrium distribution function.

In exothermic reactions  $\Delta T > 0$ , while in endothermic reactions  $\Delta T < 0$ . In the latter case, particles with energies equal to the activation energy enter the reaction, with the result that the distribution function is depleted of fast particles at initial instants of time, i.e.,  $T_n < T$ . In exothermic reactions, the excess of energy manifests itself in an increase in the number of fast particles, which is equivalent to a rise in the temperature of the distribution function, i.e.,  $T_n > T$ .

**2.1.2 Nonequilibrium surface ionization in systems that essentially depart from equilibrium:**  $\Delta T < T < T_n$ . In accordance with the definition of nonequilibrium surface ionization, the relation between the various characteristic times is given by

$$\tau_r \gg \tau_a > \tau_i. \quad (2)$$

The left inequality means that, as in Eqn (1), the reaction proceeds in a nonequilibrium manner, while the right inequality means that the ions do not have enough time to come into equilibrium with the temperature of the distribution function, a temperature higher than the surface temperature. Nonequilibrium surface ionization usually manifests itself in the

vibrationally excited states of the molecules, which may form during chemical activation, in the interaction with electromagnetic radiation, or when the kinetic energy of the particles being adsorbed is high.

By reducing the lifetime of ions at the surface in case (1) (see Section 2.1.1) we can implement situation (2), i.e., establish and measure the magnitude  $\Delta T$  of the process departure from an equilibrium one.

**2.1.3 Equilibrium surface ionization.** In the case of equilibrium systems, surface ionization is characterized by the energy relationship  $\Delta T = 0$  and the following relation for the characteristic times:

$$\tau_i \gg \tau_a \gg \tau_r.$$

Strictly speaking, this condition is insufficient for asserting that the system is in equilibrium — certain relations between microscopic parameters must also be satisfied [7]. Since what we are going to discuss deals primarily with a qualitative phenomenological approach to the description of processes of ionization of polyatomic molecules at a surface, we will limit ourselves to the above inequalities.

## 2.2 Dissociative surface ionization of polyatomic molecules

First, we must distinguish between dissociative surface ionization and dissociative ionization of particles in a gas phase. In the latter case, we have in mind the formation of fragmented dissociative ions as a result of the disintegration of an excited molecular ion that formed chiefly due to electron transitions from the ground state of the molecule [7]. In surface ionization, on the contrary, heterogeneous dissociation of the molecule first occurs and then there is surface ionization of the radicals. Such a sequence determines the yield of the products, the temperature dependences of the ion currents, and, hence, the justifiability of the term ‘dissociative surface ionization’.

The fundamental studies of surface ionization of polyatomic molecules with group-V heteroatoms, done by Zandberg and Rasulev [4], have shown that in most cases it is not the molecules of the primary beam that are ionized but, rather, the products of their chemical transformations at the surface. The yield of these products, as believed by the authors of Ref. [4], is determined by the probability of the chemical reactions following several channels ( $\gamma_i$ ) that lead to the formation of a given product. The surface-ionization mass spectrum of these polyatomic molecules consists of mass lines  $(M-H)^+$ ,  $(M-R)^+$ , and  $(M+H)^+$ , where  $M$  stands for a molecule,  $H$  for a hydrogen atom, and  $R$  for a radical. Figure 1 shows the temperature curves typical of substances belonging to these classes. Here are the characteristic features of the bell-shaped curves for  $j(T)$ : (a) a low temperature (400–600 K) of ion formation and a very small width of the peaks (100–200 K) for  $(M+H)^+$  ions; (b) a higher temperature (600–700 K) of ion formation and much wider peaks (500–800 K) for  $(M-H)^+$  ions, and (c) the highest formation temperature and a large width of the peaks for  $(M-R)^+$  ions. Experiments have shown that the  $(M-H)^+$  and  $(M-R)^+$  ions are formed in first-order reactions, and  $(M+H)^+$  ions in second-order reactions [4]. The temperature of the distribution functions of the ions coincides with the surface temperature.

One of the main postulates of the reasoning in the present article is the assumption that the above radicals are produced not in the course of various chemical reactions but in the

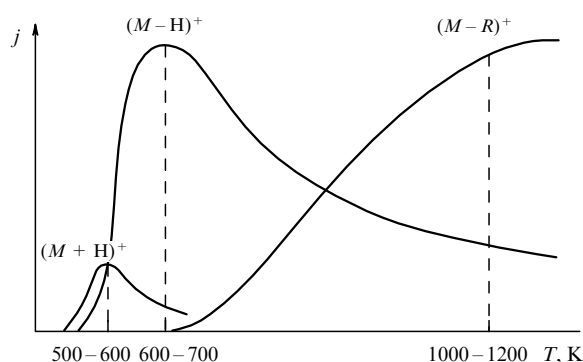
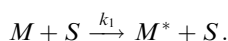


**Figure 1.** Characteristic temperature dependences of the current  $j(T)$  of polyatomic organic ions with group-V heteroatoms, forming by the mechanism of surface ionization on oxidized tungsten. (Taken from Ref. [4].)

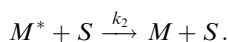
course of monomolecular disintegration of the initial molecules or fragments of multimolecular complexes at the surface. Let us discuss from this point of view the question of the order of formation reactions of disintegration products [11].

### 2.3 The kinetics of monomolecular reactions on a surface

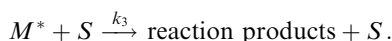
The course of monomolecular reactions in the gas phase has been thoroughly studied in several statistical theories [7, 10]. In the works [12, 13], we employed the principle of detailed balancing to justify the application of the theory of monomolecular reactions in the gas phase, which is based on transient-state theory, to describing the heterogeneous processes of disintegration of polyatomic molecules followed by ionization of the disintegration products by the surface-ionization mechanism. Here we will use another approach, in which the Lindemann scheme for monomolecular reactions [10] is applied to the interaction of molecules and a surface. The activation of a molecule  $M$  occurs when it interacts with the atoms  $S$  of the surface:



When active molecules  $M^*$  interact with the surface, they become deactivated:



In addition to becoming deactivated, the active molecules may disintegrate at the surface:



The participation of the surface at this stage stems from the catalytic nature of the heterogeneous dissociation process [10]: the adsorption energy of the disintegration products reduces the activation energy of the process. When the process proceeds steadily, the constancy of the concentration of active molecules is determined by the following condition: rate of activation = rate of deactivation + reaction rate, or

$$k_1[M] = k_2[M^*] + k_3[M^*].$$

This implies that the concentration of active molecules is given by the formula

$$[M^*] = \frac{k_1[M]}{k_2 + k_3}.$$

Then the rate of disintegration is determined from the equation

$$-\frac{\partial[M]}{\partial t} = k_3[M^*] = \frac{k_1 k_3}{k_2 + k_3} [M]. \quad (3)$$

Depending on the ratio between the rate constants of deactivation,  $k_2$ , and disintegration,  $k_3$ , we write down Eqn (3) for the two limiting cases:

(1)  $k_2 \gg k_3$ ; in this case, the lifetime  $\tau_a = k_3^{-1}$  of an active molecule is large compared to the deactivation time  $\tau_r = k_2^{-1}$ , or  $\tau_a \gg \tau_r$  (see Section 2.1.3). Equation (3) then becomes

$$-\frac{\partial[M]}{\partial t} = \frac{k_1 k_3}{k_2} [M] = k_\infty [M],$$

and it describes a first-order process. The small disintegration rate ( $k_\infty \ll k_1$ ) ensures an equilibrium energy distribution of the molecules, with the result that all the constants  $k_i$  can be written in the Arrhenius form. However, such a form does not describe the experimental temperature dependences (bell-shaped curves) of the fluxes of ions desorbing from the surface.

(2)  $k_3 \gg k_2$ , i.e.,  $\tau_r \gg \tau_a$  (see Sections 2.1.1 and 2.1.2). Then equation (3) predicts

$$-\frac{\partial[M]}{\partial t} = k_1[M] = k_0[M],$$

i.e., when active molecules have a small lifetime, the reaction is still a first-order process. This is an important result. In the gas phase, the smallness of the lifetime of active molecules compared to the time of their deactivation leads to second-order reactions which run at small pressures, i.e., nonequilibrium and equilibrium reactions in the gas phase differ in order, in contrast to reactions at a surface. We may assume that rapid molecular disintegration ( $k_0 = k_1$ ) at the surface is realized because activation of molecules occurs only at large amplitudes of vibration of the surface atoms, which statistically is a very rare process. The vibration of the surface atoms with average amplitudes leads to neither activation nor deactivation of adsorbed molecules.

### 2.4 Surface ionization of products of the monomolecular heterogeneous disintegration of molecules

When the disintegration of molecules goes rapidly and the reaction temperature does not exceed the energy of natural vibrations of the molecules ( $k_B T < h\nu$ , where  $\nu$  is the molecular vibration frequency), the statistical theory of monomolecular reactions yields an expression for the temperature dependence of the reaction rate,  $k_0(T)$ , similar to the experimental bell-shaped temperature dependences  $j(T)$  for the ions that form in the reaction [7]:

$$k_0 = B \left( \frac{E}{k_B T} \right)^b \exp \left( -\frac{E}{k_B T} \right), \quad (4)$$

where  $b$  is the effective number of the degrees of freedom [7], which according to an empirical rule amounts to one-fifth to one-third of the total number of the degrees of freedom of the molecule,  $s = 3n - 6$  [12, 13], with  $n$  being the number of atoms in the molecule, and  $E$  the excitation activation energy equal in nonequilibrium systems to the molecular dissociation activation energy. The constant  $B$  cannot be calculated because of the introduction of the parameter  $b$ .

We now describe the surface ionization of the dissociation products. Let us examine the temperature dependences of the currents of the ions that form in first-order single-channel reactions [a characteristic reaction of this type is  $M \rightarrow (M-H) + H$ ]. In surface ionization of polyatomic molecules, the strength of the measured current  $j_i$  is determined by the effective flux  $g_i$  of radicals from the surface [4] and the surface ionization coefficient  $\beta_i$  of these radicals:  $j_i = eg_i \beta_i$ .

The magnitude of the fluxes is determined either from the degree of dissociation,  $\gamma_i = g_i/g$ , with a constant flux  $g$  of molecules to the surface and a single reaction channel or from the concentration  $n^*$  of the particles at the surface and the rate constant  $k_0$ :  $g_i = k_0 n^*$ . It has proved convenient to express the concentration of particles in terms of the flux of particles to the surface via the formula known from the perfect-gas kinetic theory:  $g = n_g^* [k_B T_g / (2\pi m)]^{1/2}$ , where  $n_g^*$  and  $T_g$  are the parameters of the gas phase. In the steady-state regime, a certain concentration  $n^*$  of particles establishes itself at the surface, a concentration that ensures a flux from the surface equal to  $g$ .

Then for the ion current of the products of monomolecular disintegration for the case  $\beta_i = \alpha_i \ll 1$  (in what follows we drop the subscript  $i$  to make the notation compact) we have

$$j = ek_0 n^* \beta = egB^* \left( \frac{E}{k_B T} \right)^b \exp \frac{\Pi - E}{k_B T}, \quad (5)$$

where  $\Pi = e(\varphi - V + \sqrt{eF})$  is the surface-ionization term [2],  $\alpha = \beta/(1 - \beta)$  is the degree of surface ionization,  $e\varphi$  is the work function of the surface,  $eV$  is the radical's ionization potential,  $F$  is the electric field strength at the surface of the emitter, and  $B^*$  is a constant. The condition  $\alpha \ll 1$  is met when  $|\Pi| \gg k_B T$ , i.e., in the case of surface ionization of hardly ionizable substances [2], which is what we discuss below.

Two new parameters, missing in surface-ionization theory, have been introduced in Eqn (5):  $E$ , the dissociation activation energy at the surface, and  $b$ , the number of active degrees of freedom participating in the dissociation process. Let us discuss the possibility of depending these parameters on the electric field strength.

Korol' et al. [14] showed that the bond-rupture energy depends on the electric field strength  $F$  in such a way that as the field varies from  $10^4$  to  $6 \times 10^6$  V cm $^{-1}$  the 3-eV binding energy drops by 0.04–0.05 eV. Since this magnitude coincides with the accuracy of our method, we can assume that within this range of field strengths the energy  $E$  is independent of  $F$ .

The idea of effective, or active, degrees of freedom is related to the specific features of statistical theories of monomolecular reactions. Such theories are based on the fluctuational nature of the energy redistribution among the degrees of freedom of the molecule that is modelled by a set of harmonic oscillators, actually meaning that the anharmonicity ensuring the interaction of the reaction coordinate with all vibrational degrees of freedom is taken into account implicitly.

However, in interpreting the experimental data one is forced in most cases to use an effective number of oscillators that is smaller than the true number of vibrational degrees of freedom. This means that the interaction of the reaction coordinate with the degrees of freedom differs from one degree of freedom to another rather than being unique for all degrees of freedom. This suggests that even small variations in the oscillator energy and, hence, in the interac-

tion between the oscillators may result in changing the effective number of the degrees of freedom. It can be assumed that when electric fields with the intensity of about  $\sim 10^6$  V cm $^{-1}$  act on the system, these variations are caused by (a) the Stark effect leading to a shift in and splitting of the energy levels in a molecule, and (b) the steric factor which manifests itself in a change in the orientation of molecules with respect to the surface and brings about a shift in the energy levels caused by a change in the adsorption interaction.

Moreover, one must bear in mind the possibility of manifesting, in electric fields, the correction  $\delta$  introduced into the exponent in Eqn (5) by Zandberg and Ionov [2] to take into account the work of the rapidly decreasing van der Waals forces of attraction of an ion to a surface and the possible deviation of this interaction from the Coulomb interaction. However, since the functions  $b(F)$  and  $\delta(F)$  may be represented only in empirical form, for the time being (until Section 5) we assume that only  $b$  depends on  $F$ .

## 2.5 Surface ionization in the monomolecular disintegration of fragments of a multimolecular complex

In addition to very broad peaks in the temperature dependences  $j(T)$  at relatively high temperatures of the surface, discussed in Section 2.4, at low temperatures (400–600 K) there are very narrow peaks in the  $j$  vs.  $T$  dependence (with half-widths ranging from 100 to 200 K), for example, in the case of associative ions [4] and in ionizing dimers [15]. The same narrow peaks were measured by us in studying the surface ionization of products of the exothermic disintegration of acetone peroxide. The number  $b^*$  of the degrees of freedom of the ions, determined by the method that will be discussed in Section 4.2, was found to form narrow temperature peaks and turned out to be 10 times higher than the number of the total degrees of freedom of a given particle. Such a situation emerges if the particles are formed during disintegration of a multimolecular complex whose numerous degrees of freedom participate in this process [16].

The formation of multimolecular complexes at low surface temperatures is a characteristic feature of two-dimensional gases [17]. Since the dissociation, substitution, and association reactions of the molecules comprising a complex may run in such a complex, we may think of it as an activated multimolecular complex. Without writing down the full expression for the rate constant  $k_N$  of the reaction of dissociation of the multimolecular complex  $M_N = M^1 + \dots + M^N$  [16], we present only the temperature dependence  $k_N(T)$ . What we are interested in is the disintegration of such a complex at a surface. The number of degrees of freedom of the transient complex at the surface is smaller than in the gas phase, since the rotation of the complex at the surface is frozen and only two degrees of freedom remain free for translational motion. The individual molecules that form the complex also have two translational degrees of freedom and, in addition, one rotational degree of freedom which corresponds to the adsorption bond. We showed in Ref. [18] that if one allows for all this and the fact that  $h\nu > k_B T$  (where  $\nu$  is the frequency of the natural vibrations of the molecule), which follows from the experimental conditions, then the expression for  $k_N(T)$  acquires the simple form

$$k_N(T) \approx G \left( \frac{1}{k_B T} \right)^{(3N-4)/2} \exp \left( -\frac{E_N}{k_B T} \right),$$

where  $N$  is the number of molecules in the complex,  $E_N$  is the disintegration activation energy of the complex, and  $G$  is a temperature-independent constant. Notice that the exponent of the pre-exponential factor is twice as small for the process of monomolecular disintegration of a multimolecular complex at a surface [18] as it is in the bulky case [16].

Now we turn to the process of monomolecular disintegration of a fragment of a multimolecular complex, a process that is naturally accompanied by the disintegration of the entire complex. Let us show that the temperature dependence of the rate constant  $k_0$  of a monomolecular reaction is enhanced because of the contribution from the temperature dependence of the disintegration rate constant  $k_N$  of the entire complex. The physics of the process amounts to the following: the multimolecular complex stores considerable amounts of energy in its numerous bonds; this energy may be statistically redistributed and may concentrate primarily in one of the fragments of the molecular complex. Hence, disintegration of the multimolecular complex ( $k_N$ ) and monomolecular disintegration of a single fragment ( $k_0$ ) occur simultaneously. Since processes in the multimolecular complex are the primary ones, its rate constant  $k_N$  enters as the base [instead of  $(E/k_B T)$  in Eqn (4)] of the power function of the pre-exponential factor in the rate constant  $k_0$  of the monomolecular reaction. Then for the temperature dependence of the rate constant of the monomolecular disintegration of a fragment of a multimolecular complex we arrive at the following expression (see Ref. [18]):

$$k_0^N \approx C \left[ \left( \frac{1}{k_B T} \right)^{(3N-4)/2} \exp \left( -\frac{E_N}{k_B T} \right) \right]^b \exp \left( -\frac{E}{k_B T} \right),$$

from which it follows that the probability of the entire complex decomposing because of the energy stored in the numerous bonds in the complex contributes to the effective degree of freedom ( $b$ ) of each fragment. The reader will recall that in this formula  $E$  is the activation energy of the disintegration of a fragment, and  $E_N$  is the activation energy of the entire complex.

By analogy with the monomolecular decay of a single molecule [see Eqn (5)], we can write down the formulas for the temperature dependence of the ion current in the surface ionization of a fragment of a heterogeneous multimolecular complex:

$$\begin{aligned} j_N &= e k_0^N n^* \beta \\ &\approx e g D \left[ \left( \frac{1}{k_B T} \right)^{(3N-4)/2} \exp \left( -\frac{E_N}{k_B T} \right) \right]^b \exp \frac{\Pi - E}{k_B T} \\ &= e g D \left( \frac{1}{k_B T} \right)^{(3N-4)b/2} \exp \frac{\Pi - E - b E_N}{k_B T}, \end{aligned} \quad (6)$$

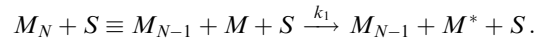
where  $D$  is a constant incorporating the constant  $C$ .

All this suggests that at  $N \sim 10$  the number of effective degrees of freedom participating in the disintegration of the fragment [i.e.,  $b^* = b(3N-4)/2$ , similar to  $b$  in expression (5)] increases by a factor greater than 10, which leads to a small half-width of the bell-shaped temperature dependence of the ion flux from the given fragment.

## 2.6 The formation kinetics of fragments of a multimolecular complex

Let us examine the equations that describe the excitation and monomolecular disintegration of a fragment or molecule of a

multimolecular complex [11]. Since according to the basic postulate of chemical kinetics the rate of disintegration of a molecule is proportional to the concentration of these molecules, we must isolate the molecule  $M$  in the multimolecular complex  $M_N = M^1 + \dots + M^N$ . Thus, the process of excitation of a fragment  $M$  of a multimolecular complex  $M_N$  at a surface can be described as follows:



Using equations similar to the equations governing deactivation and disintegration of single molecules (see Section 2.3), we arrive (see Ref. [11]) at an equation for the reaction rate in steady-state process for a multimolecular complex:

$$-\frac{\partial[M]}{\partial t} = k_3[M^*] = \frac{k_1 k_3}{k_2 + k_3} [M] [M_{N-1}].$$

We see that the monomolecular disintegration of a fragment of a multimolecular complex proceeds as a second-order reaction. Experiments with associative ions  $(M + H)^+$  have revealed that the reaction of the formation of associative ions belongs to the second-order ones [4]. Here, the injection of hydrogen, deuterium, and water into the reaction zone did not lead to a rise in current, i.e., the second order of the reaction stems not from the attachment of a hydrogen atom to the molecule but probably from the separation of an associative fragment from the multimolecular complex. This fact and also the first order of the reaction of disintegration of a single molecule established in the experiments described in Ref. [13] support the kinetic schemes discussed in Sections 2.3 and 2.6.

We point once more to the important conclusion that the monomolecular disintegration at a solid surface constitutes a nonequilibrium process, with the result that it is described by a nonequilibrium distribution function. When the lifetime of the ions at the surface is large, they come into equilibrium with the surface temperature, so that the ionization of molecules and radicals can be described by the surface-ionization theory. However, the yield of the reaction products is determined by the nonequilibrium distribution function.

## 3. Nonequilibrium surface ionization. General ideas

We introduced the term ‘nonequilibrium surface ionization’ in 1988 in the work [19], so as to quantitatively describe surface ionization in systems with a significant departure from equilibrium. Energy-saturated compounds, in which the products of heterogeneous disintegration become ionized, belong to such systems. Describing them, as noted in the Introduction, requires not one (as in the equilibrium case) but two or more energy parameters (distribution functions) [8].

### 3.1 Statistical derivation of the degree of nonequilibrium surface ionization

Even without specifying explicitly the source of departure from equilibrium, we can state that the particles desorbing from the surface of an emitter maintained at the temperature  $T$  have a distribution function with a characteristic temperature  $T_n > T$ . Then the charge state of the emitted particles is determined by the occupancy of the energy states of the

emitter, i.e., the surface temperature  $T$ , while the probability of particle emission is determined by the temperature  $T_n$ . The quantity measured in experiments,  $\Delta T = T_n - T$ , characterizes the extent to which the temperature of the distribution function of the ions being desorbed exceeds the surface temperature. Following the statistical derivation of the formula for the degree of surface ionization [20], we can write down the ratio of the probabilities of transforming a particle being desorbed into an ion or a neutral particle as follows:

$$\frac{w^{+'}}{w^{0'}} = A \exp \frac{e(\varphi - V^*)}{k_B T} = A \exp \frac{e(\varphi - V) + \lambda_+ - \lambda_0}{k_B T}, \quad (7)$$

where  $A$  is the ratio of the partition functions of the ionic and neutral states of the particle,  $eV^*$  is the ionization potential of an adsorbed particle at the critical distance of charge exchange, and  $\lambda_+$  and  $\lambda_0$  are the works of evaporation of ions and neutral particles, related to  $V$  and  $V^*$  by the formula

$$eV^* = \lambda_0 - \lambda_+ + eV, \quad (8)$$

derived from the circular thermodynamic cycle [20]. For ions and neutral particles characterized by the temperature  $T_n$ , the ratio of the probabilities of their kinetic energy exceeding  $\lambda_+$  and  $\lambda_0$  is expressed, accordingly, in the form

$$\frac{w_\lambda^+}{w_\lambda^0} = \exp \frac{\lambda_0 - \lambda_+}{k_B T_n}. \quad (9)$$

Then the degree of nonequilibrium surface ionization, equal to the ratio of the probabilities of ions and neutral particles evaporating, can be written down as the product of Eqns (7) and (9):

$$\alpha_n = \frac{w^+}{w^0} = \frac{w^{+'}}{w^{0'}} \frac{w_\lambda^+}{w_\lambda^0} = A \exp \left[ \frac{e(\varphi - V)}{k_B T} + (\lambda_+ - \lambda_0) \left( \frac{1}{k_B T} - \frac{1}{k_B T_n} \right) \right]. \quad (10)$$

Using the definition of  $\Delta T$  and formula (8) and representing the cofactors in the last term inside square brackets in the form

$$\frac{1}{k_B T} - \frac{1}{k_B T_n} = \frac{1}{k_B T} \left( 1 - \frac{T}{T_n} \right) = \frac{1}{k_B T} \frac{\Delta T}{T_n},$$

$$\lambda_+ - \lambda_0 = e(V - V^*) = e(\varphi - V^*) - e(\varphi - V),$$

we arrive at the desired degree

$$\alpha_n = A \exp \frac{e(\varphi - V)}{k_B T_n} \left[ 1 + \frac{\varphi - V^*}{\varphi - V} \frac{\Delta T}{T} \right]. \quad (11)$$

Both cofactors of the second term inside the square brackets in expression (11) are smaller than unity. Indeed,  $\Delta T/T < 1$ , and since  $V > V^* > \varphi$ , we have

$$\frac{\varphi - V^*}{\varphi - V} < 1.$$

Ignoring the second term inside the square brackets on the right-hand side of Eqn (10) in view of its smallness compared to unity, we arrive at an expression for  $\alpha_n/\alpha_r$  that can be compared to  $\alpha_{\text{exp}}/\alpha_r$ , where  $\alpha_{\text{exp}}$  is the degree of

nonequilibrium surface ionization measured in an experiment with the particles in question:

$$\frac{\alpha_n}{\alpha_r} \approx \exp \left[ \frac{e(\varphi - V)}{k_B T_n} \left( -\frac{\Delta T}{T} \right) \right]. \quad (12)$$

For particles whose ionization proves arduous [ $e(V - \varphi) \gg k_B T$ ], this ratio is greater than unity if  $\Delta T > 0$  (exothermic processes) and smaller than unity if  $\Delta T < 0$  (endothermic processes). In the equilibrium case ( $\Delta T = 0$ ), the ratio (12) is equal to unity.

Formally, the relations derived have to describe the case of unaccommodated ionization with desorption of both hot,  $\Delta T > 0$ , and (at least theoretically) cold,  $\Delta T < 0$ , ions. Indeed, N I Ionov examined this problem (see Ref. [2]) and derived a formula for the degree of ionization for the elastic collision of particles with a surface,  $\alpha_{\text{el}}$ , similar to Eqn (10). The expression for  $\alpha_{\text{el}}$  in Ref. [2] can also be rearranged to the form similar to Eqn (12), which is convenient for making estimates (see Ref. [21]). The fact that the formulas are identical can be explained by the identical nature of the initial ideas on the basis of which these expressions were independently derived.

### 3.2 Statistical derivation of the degree of nonequilibrium surface ionization in an electric field

In the presence of an electric field accelerating ions, the work of ion desorption,  $\lambda_+$ , decreases by

$$\Delta \lambda(F) = \lambda_+ - \lambda_+^F, \quad (13)$$

where  $\lambda_+^F$  is the work of ion desorption in the electric field. At the same time, in the field, at a distance  $x_c$  from the surface at which electron exchange between particle and surface ceases, the counting-off level of the vacuum potential is raised by  $eFx_c$  [2]. Accordingly, the electronic level of the neutral particle also shifts that may be thought of as an increase in the effective work function of the surface by the same quantity. Then the quantity  $e(V^* - \varphi)$ , which determines the probability of an electron moving from an adsorbed particle into the emitter, is replaced by  $e(V^* - \varphi - Fx_c)$ , while the ratio of the probabilities of the adsorbed particle transforming into an ion or neutral particle in the electric field can be written in the following form

$$\frac{w^{+'}}{w^{0'}} = A \exp \left[ \frac{e(\varphi - V^* + Fx_c)}{k_B T} \right]. \quad (14)$$

To reduce formula (14) to expression (7) we must find  $\lambda_+$  from relationship (13).

An expression for  $\Delta \lambda$  can be obtained if we integrate the differences of the forces acting on the ion over the coordinate from the critical distance  $x_c$  to  $x = \infty$  at  $F = 0$ , and to  $x = x_0$  for  $F \neq 0$ , where  $x_0$  is the distance at which the force  $eF(x_0)$  of the external field acting on the ion is balanced by the force of mirror reflection. Substituting the result of integration [22]

$$\Delta \lambda = \frac{e^2}{4x_0} + eFx_0 - eFx_c \quad (15)$$

into expression (13), we arrive at an equation for  $\lambda_+$ . Substituting  $\lambda_+$  into relationship (8), using the equality  $e^2/(4x_0) + eFx_0 = e\sqrt{eF}$  [2], and assuming that  $\lambda_0^F = \lambda_0$  for neutral particles in the range of the used field strengths, we

can write Eqn (14) in a form similar to Eqn (7):

$$\frac{w^{+'}}{w^{0'}} = A \exp \left[ \frac{\Pi}{k_B T} + \frac{\lambda_+^F - \lambda_0^F}{k_B T} \right], \quad (16)$$

where  $\Pi = e(\varphi - V + \sqrt{eF})$  [2].

Following the logic used in deriving formula (11), we arrive at [23]

$$\alpha_n = A \exp \left( \frac{\Pi}{k_B T_n} \right) \left[ 1 + \frac{\varphi + Fx_c - V^*}{\Pi} \frac{\Delta T}{T} \right]. \quad (17)$$

At  $F = 0$ , the last equation reduces to expression (11) for  $\alpha_n$ .

In approximation (12), the ratio  $\alpha_n/\alpha_r$  with allowance for an electric field can be written down as follows:

$$\frac{\alpha_n}{\alpha_r} = \exp \frac{\Pi}{k_B T_n} \left( -\frac{\Delta T}{T} \right). \quad (18)$$

### 3.3 Nonequilibrium surface ionization of fragments of multimolecular complexes

The formation of ions of fragments of a multimolecular complex by the mechanism of nonequilibrium surface ionization in the case of essentially nonequilibrium processes initiated by exothermic reactions in the complex differs substantially from a similar process [18] under surface ionization. Let us discuss the possible scheme of the process, singling out two stages in it.

We assume that the formation and the first stage in the disintegration (exothermic transformation) of the complex proceed at the temperature  $T$  equal to the surface temperature. In the transformation of the transient multimolecular complex at the expense of the energy liberated in the exothermic reaction, vibrationally excited states emerge (the second stage). After the complex has finished transforming, its disintegration and separation, ionization, and desorption of fragments occur in the vibrationally excited states which are characterized by the temperature  $T_n$  of the energy distribution function.

A rigorous mathematical description of these processes is hardly possible if we remain within the scope of the ideas developed here. Therefore, first we write down the equation for the current of the ions being desorbed, allowing mainly for the first and (partially) the second stages in the process, i.e., we describe the formation and disintegration of the complex by using the temperature  $T$  [the expression inside the square brackets in Eqn (6) is the rate constant of formation and disintegration of a multimolecular complex], while the ionization and desorption of the fragments (the exponent) are described by the temperature  $T_n$ :

$$j_N \approx egD \left[ \left( \frac{1}{k_B T} \right)^{(3N-4)/2} \exp \left( -\frac{E_N}{k_B T} \right) \right]^b \exp \frac{\Pi - E}{k_B T_n}.$$

For the last equation to correctly describe the experimental temperature dependence, we must introduce the unique temperature  $T_n = T + \Delta T$  and write it down in the form

$$j_N \approx egD \left[ \left( \frac{1}{k_B T_n} \frac{T_n}{T} \right)^{(3N-4)/2} \exp \left( -\frac{E_N}{k_B T_n} \frac{T_n}{T} \right) \right]^b \times \exp \frac{\Pi - E}{k_B T_n}.$$

Since  $\Delta T/T < 1$  and  $\Delta T(3N-4)/2T > 1$ , we can replace  $T$  in the denominator with  $T_n$  and, assuming that  $T_n/T = m = \text{const}$ , we can derive the following approximate formula for the power-term base:

$$\left[ \frac{1}{k_B T_n} \left( 1 + \frac{\Delta T}{T} \right) \right]^{(3N-4)/2} \approx \left( \frac{1}{k_B T_n} \right)^{(3N-4)/2} \frac{\Delta T(3N-4)/2}{T} \approx B \left( \frac{1}{k_B T_n} \right)^{(3N-4)/2+1},$$

while the exponent assumes the form

$$\frac{E_N}{k_B T_n} \frac{T_n}{T} \approx \frac{mE_N}{k_B T_n}.$$

By assuming that  $T_n/T = m = \text{const}$  we somewhat decrease the slope of the initial exponential curve, which corresponds to a partial increase in the role that  $T_n$  plays (in the same way as the replacement of  $T$  with the temperature  $T_n$  in the previous formula) in accordance with the fact that in the second stage the complex also acquires the temperature  $T_n$ .

Thus, the result is given by

$$j_N(T_n, F) \approx egA \left( \frac{1}{k_B T_n} \right)^{(3N-2)b/2} \exp \frac{\Pi - E - mE_N b}{k_B T_n}. \quad (19)$$

## 4. Method

### 4.1 Surface-ionization field mass spectrometry

The study of time variations in the distribution functions of the products of heterogeneous reactions resulted in the creation of a new first-rate method — surface-ionization field mass spectrometry.

The idea of the method consists in controllable variation (within a broad range) of the lifetimes of ions on a surface by reducing the height of the Schottky barrier through the application of an electric field, which changes the energy of the desorbed ions by a factor of 100.

The use of the mass-spectrometry method in surface-ionization studies of polyatomic molecules placed in electric fields is necessary, but requires the energy of the ions to remain constant as they enter the mass spectrometer. Thus, implementing the method requires the surface-ionization source of ions to be achromatic within a broad range of energies of the desorbed ions. The achromaticity condition is equivalent to the requirement that the geometry of the ion beam remains constant as one of the potentials of the electron-optical system changes by a factor of about 100. This can be achieved only if the electron immersion lenses operate in the ultimate regime, i.e., when the ratio of the potentials on the lens tends to zero with one of the potentials increasing. Indeed, if the ratio of the initial potentials in such a regime is close to zero, any further increase in one of the potentials within any region only slowly drives the ratio to zero, with the result that the optical characteristics of the system change little. Such a decelerating immersion lens is, actually, an inverted immersion objective, for which, as is known, the focusing of the image at small distances between the emitter and the first electrode depends very little on the ratio of their potentials [24].

Thus, the electron-optical schematic diagram (Fig. 2) of the ion source must consist of an emitter, a suppressor grid, an



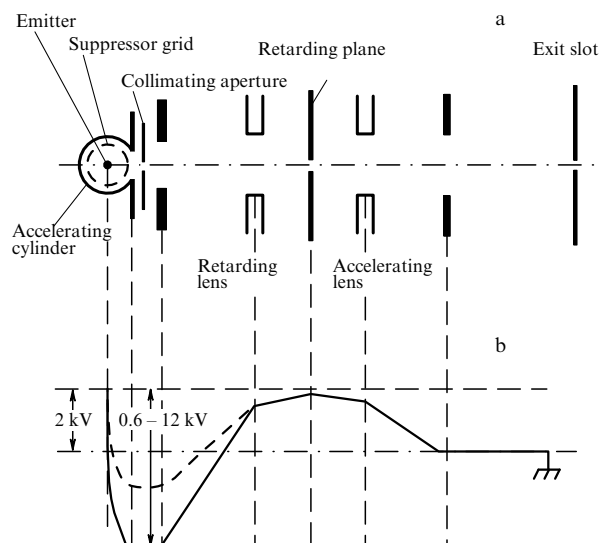


**Figure 2.** (a) The schematic diagram of an achromatic field surface-ionization source of ions. (b) The electric potentials on the electrodes of the source that accelerate positive ions. The output ion energy is 2 kV. The range of potentials on the accelerating cylinder corresponds to a change in the strength of the electric field near the emitter from  $2 \times 10^5$  to  $3.4 \times 10^6 \text{ V cm}^{-1}$ .

ion-accelerating cylindrical electrode which sets up an electric field that varies within a certain predetermined range, electrodes that retard the ion beam down to the initial (thermal) energy and generate an intermediate image, and, finally, electrodes that accelerate the ions to the constant energy needed for the operation of the mass spectrometer and focus the intermediate image onto the entrance slot of the mass spectrometer [25]. The design of the source was based on that of an electron-optical system of an energy analyzer with an intermediate image (the description and design can be found in Ref. [26]). Such an electron-optical system must, first, guarantee that the optical characteristics remain the same when one of the potentials in the system varies or, what amounts to the same thing, when the energy of the beam at the entrance slot of the energy analyzer changes, and, second, serve its purpose — that is, ensure an energy analysis of the beam.

To estimate the resolving power of the analyzer, Simpson [26] provided the following expression

$$\frac{\Delta U}{U} = \frac{\Delta E}{E} = M_a^{-2} \sin^2 \Theta. \quad (20)$$

Clearly, the resolving power  $E/\Delta E$  of the energy analyzer remains constant as the beam energy  $E$  changes, since it is determined by the magnification  $M_a$  of the system and the entrance aperture  $\Theta$ . Here,  $\Delta E$  ( $\Delta U$ ) is the minimum energy at which a beam of particles with the initial energy  $E$  (or, accordingly,  $U$ ) can still be focused in the retarding plane. Since the analyzer employed is an integral one, to determine  $\Delta U$  we can use the retarding field method (delay curve method) in which, as is known, the relative variation  $\Delta T/T$  in the temperature of the ion distribution function corresponds to the same relative variation  $\Delta U/U_d$  in the retarding potential [2].

When the necessary accuracy in determining  $\Delta T$  on the basis of formula (20) was specified and the essential relationships from Refs [26, 27] were employed, the cylindrical

and axisymmetric variants of the lens systems for the ion sources, which overlapped field strength ranges of  $3 \times 10^5 - 8 \times 10^6 \text{ V cm}^{-1}$  [28] and  $10^7 - 8 \times 10^8 \text{ V cm}^{-1}$  [29], were calculated [9] and implemented. To increase the energy resolution in the cylindrical variant, we added a retarding immersion lens operating in the proportional mode and lowering the energy of the ion beam at the entrance to the energy analyzer by a factor of three. This made it possible to reach an experimental resolution of  $\pm(30-50) \text{ K}$  in  $\Delta T$ , which corresponded to roughly 0.01 eV, keeping the analyzer in the same operational mode. At an average kinetic energy of the ion beam of roughly  $\sim 10^3 \text{ eV}$ , the resolving power turns out to be at a level of about  $10^5$ .

A pure or oxidized tungsten filament 5 or 10  $\mu\text{m}$  in diameter served as an emitter in our experiments. This allowed us to calculate the strength of the electric field near the emitter's surface and guaranteed that there would be no field migration and that the emitter's area would be large.

The source was placed inside a stainless steel chamber which could be heated. Before each experiment, the emitter was cleaned by heating it to a high temperature in a vacuum ( $10^{-9}$  Torr) up to the filament's recrystallization point. The filament prepared in this way had the greatest possible work function of ions in both the 'metallic' ( $\phi = 4.9-5.0 \text{ eV}$ ) and the 'oxidized' ( $\phi = 6.6-6.8 \text{ eV}$ ) states, which made it possible to reliably record the ion currents of substances with an ionization potential up to 8.5–9 eV using a filament source. If necessary, thick layers of oxides were grown on the tungsten filament by a method proposed in Refs [30–32]. This ensured a stable emission of ions of the admitted substances in the course of a relatively long time interval, which suggests that the composition of the emitter's surface remained the same during the experiments. When emission weakened, the oxide layer restored its properties after the filament was cleaned by high-temperature heating. In the experiments, the temperature of the pure filament was kept at 1800 K, and that of the oxidized filament at 1150 K. The pressure of the admitted substances amounted to  $10^{-7}$  Torr. The ion beam from the source was sent through a static sector ( $60^\circ$ ) magnetic analyzer whose radius was 200 mm. The ions were registered in the pulse counting mode. The resolving power  $R$  of the mass spectrometer amounted to 200. The residual pressure in the vacuum chamber was not higher than  $10^{-9}$  Torr. To monitor the residual gases and purity of the admitted substances, an electron-impact source with an imaginary ion image was placed behind the exit slot of the field source. The image was projected onto this slot, i.e., the entrance slot of the mass spectrometer [9], which guaranteed high sensitivity for standard resolution and did not disrupt the design of the field source.

To calibrate the device and to determine the work function of the emitter, the vaporizers of Cs, In, and Bi atoms were placed in the source.

In studying the reactions of disintegration of polyatomic molecules consisting of three or more types of atoms, high-resolution mass spectrometry should be used in the stage when the disintegration products are identified. To this end, a high-resolution magnetic-resonance mass spectrometer with  $R = (2-3) \times 10^4$  was employed in our experiments [33].

#### 4.2 The shape of the temperature dependences of the ion current as a function of the electric field strength

In Section 2.4 we derived expression (5) for the current of the products of the disintegration of polyatomic

molecules. To analyze and determine the parameters ( $V$ ,  $b$ , and  $E$ ) of the process, we rewrite formula (5) in a more compact form by introducing the notation  $x = 1/k_B T$  and  $c = e(\varphi - V + \sqrt{eF}) - E = \Pi - E$ :

$$j = B' x^b \exp(cx), \quad (21)$$

where  $B'$  contains quantities that depend neither on  $T$  nor on  $F$ ;  $b > 0$ , and  $c < 0$ .

By nullifying the first derivative  $j'_x$  we can find the dependence of the temperature of the curve's peak, i.e.,  $k_B T_{\max}$ , on the surface-ionization parameters:

$$k_B T_{\max} = -\frac{c}{b} = \frac{E - \Pi}{b}. \quad (22)$$

Clearly, the maximum of the temperature dependence at  $b = \text{const}$  and  $E = \text{const}$  must shift toward lower temperatures in proportion to  $\sqrt{F}$ . However, experimental data suggest that the dependence of  $k_B T_{\max}$  on  $F$  is more complicated, which may be due to the dependence of both  $b$  and  $\Pi$  on  $F$ , caused by the correction  $\delta$  (see Section 2.4). To simplify the notation we limit ourselves to a single empirical dependence,  $b(F)$ .

The inflection points in dependence (21) can be found by nullifying the second derivative  $j''_{xx}$ :

$$k_B T_{1,2} = -\frac{c}{b \pm \sqrt{b}} = \frac{E - \Pi}{b \pm \sqrt{b}}. \quad (23)$$

Using Eqns (23) and (22), we can calculate the width of the bell-shaped curve from the ordinates of the inflection points, expressing it in terms of  $k_B T_{\max}$ :

$$\delta k_B T = \frac{2k_B T_{\max} b}{(b - 1)\sqrt{b}}. \quad (24)$$

Equation (24) implies that the width of the temperature interval between the inflection points of the temperature curves decreases as  $T_{\max}$  moves toward the low-temperature region, and increases in the opposite direction. Finally, from formula (22) and one of equations (23) we can find the number of effective degrees of freedom of the molecule:

$$b = \left( \frac{T_{\max}}{T_1} - 1 \right)^{-2}. \quad (25)$$

The empirically established function  $b(F)$  should manifest itself in the field dependence of the ion currents,  $j(F)$ , i.e., make this dependence deviate from the Schottky-like [2]. The dependences  $j(F)$  for currents of monatomic ions at  $T = \text{const}$  are usually built (see Ref. [34]) in the  $(\ln j, \sqrt{F})$  coordinates:

$$\ln \frac{j_1}{j_2} = \frac{e\sqrt{e}}{k_B T} (\sqrt{F_1} - \sqrt{F_2}).$$

Expression (5) for the logarithm of the ratio of currents of polyatomic ions yields

$$\ln \frac{j_1}{j_2} = \frac{e\sqrt{e}}{k_B T} (\sqrt{F_1} - \sqrt{F_2}) + [b(F_1) - b(F_2)] \ln \frac{E}{k_B T}. \quad (26)$$

Comparing these two equations, we see that the slopes of the plots  $(T_F)$  of the field dependences of the currents of

polyatomic and monatomic ions,  $j(\sqrt{F})$ , will be determined by the difference  $b(F_1) - b(F_2)$ .

We can find  $E$  from expression (26) for the logarithm of the ratio of currents for two different values of the field strength,  $F_1 > F_2$ . Taking the antilogarithm of an appropriate number yields

$$E = k_B T \exp \frac{\ln(j_1/j_2) - e\sqrt{e}/(k_B T)(\sqrt{F_1} - \sqrt{F_2})}{b_1 - b_2}. \quad (27)$$

Finding  $E$  from expression (27) and  $b$  from expression (25) and using experimental values of  $F$  and  $\varphi$ , we can calculate, via formula (22), the ionization potential  $V$  of a polyatomic radical.

The equation for the current of ions of fragments of a multimolecular complex can be used to derive equations similar to relationships (22) and (25) for determining  $b^*$ ,  $V$ ,  $N$ , and  $E_N$  from the experimental values of  $T_{\max}$  (the temperature of the maximum) and  $T_1$  (the temperature of an inflection point) for the curve  $j_N(T, F)$ :

$$b^* k_B T_{\max} = eV + bE_N + E - e\varphi - e\sqrt{eF}, \quad (28)$$

$$b^* = \left( \frac{T_{\max}}{T_1} - 1 \right)^{-2} = \frac{b(3N - 4)}{2}. \quad (29)$$

The values of  $\varphi$  and  $F$  can also be found from experiments. Actually, here  $b$  is a fitting parameter, since it is chosen within a range from one-fifth to one-third of the total number of degrees of freedom of the particle in question. Then the value of  $N$  can be determined with an accuracy of  $\pm(10-15)\%$ . Unfortunately, the parameters  $E$ ,  $E_N$ , and  $V$  cannot be determined independently. The order of magnitude of the quantity  $E$  can be compared with the values of the heterogeneous dissociation activation energy determined from formula (27). If the particle's ionization potential is known,  $E_N$  can be found from Eqn (28). If the ionization potential is not known, the parameters  $E_N$  and  $V$  of a multimolecular complex can be determined only with an accuracy of about 20% since the ionization potentials of substances belonging to certain classes have a spread of about  $\pm(1.5-2)$  eV.

In concluding this section, we write down the formulas for estimating the parameters  $b_n^*$ ,  $V$ , and  $N$  of a multimolecular complex in a state just before the formation and ionization of the fragments of the complex by the mechanism of nonequilibrium surface ionization with the temperature  $T_n$  (see Section 3.3), formulas that are similar to Eqns (28) and (29):

$$b_n^* k_B T_n^{\max} = eV + E + mE_N b - e\varphi - e\sqrt{eF}, \quad (30)$$

$$b_n^* = \frac{(3N - 2)b}{2} = \left( \frac{T_n^{\max}}{T_n^1} - 1 \right)^{-2}. \quad (31)$$

When formulas (30) and (31) are utilized in calculations, the temperature axis  $T$  in the experimental temperature curves for the ion current is replaced with the axis  $T_n = T + \Delta T$ .

#### 4.3 The lifetime and the energy distribution function of ions as functions of the electric field strength

Let us analyze the dependences of  $\tau_i$  and  $\Delta T$  on  $F$ . We write down in an analytical form the relative variation in the lifetime  $\tau_i$  of dissociated polyatomic ions as a function of  $F$ .

The ion desorption probability  $w$  is inversely proportional to the ion lifetime  $\tau_i$  on the surface and can be written as

follows (see Ref. [2]):

$$w = \frac{1}{\tau_i} = C \exp \left( -\frac{I^+(F)}{k_B T} \right),$$

where  $C$  is the pre-exponential factor, and  $I^+$  is the isothermal ion desorption heat.

We obtain an expression for the relative variation in  $I^+(F)$  by setting up an equation for the case of dissociative ions that is similar to the Schottky relation for atoms [35]:  $e(\varphi - V + \sqrt{eF}) = I^0(F) - I^+(F)$ . To this end, we take Eqn (5) for the current of polyatomic ions, in which we incorporate in the exponent all the  $F$ -dependent terms:

$$j = egB \exp \frac{\Pi - E + k_B T b(F) \ln(E/k_B T)}{k_B T}. \quad (32)$$

Making the numerator in the exponent of formula (32) equal to the difference between the isothermal heats, we arrive at an expression for  $I^+(F)$ :

$$-I^+(F) = \Pi - E + k_B T b(F) \ln \left( \frac{E}{k_B T} \right) - I^0(F)$$

or for  $w$  in the expanded form

$$w \sim \left( \frac{E}{k_B T} \right)^{b(F)} \exp \left( \frac{e(\varphi + \sqrt{eF} - V) - E - I^0(F)}{k_B T} \right).$$

Note that we have dropped the pre-exponential factors that do not depend on  $F$ , since in what follows we examine the relative variations in  $w$ .

Ignoring, due to their smallness, the variations in the heat of desorption of neutral particles in the presence of an electric field,  $I^0(F)$ , compared to variations in the ion desorption heat  $I^+(F)$ , we arrive at a formula for the relative variation of the ion lifetime as the field strength increases from  $F_1$  to  $F_i$ :

$$\frac{w_i}{w_1} = \frac{\tau_{i1}}{\tau_{ii}} = \left( \frac{E}{k_B T} \right)^{\Delta b(F)} \exp \left( \frac{e(\sqrt{eF_i} - \sqrt{eF_1})}{k_B T} \right), \quad (33)$$

where  $\Delta b = b(F_i) - b(F_1)$ .

Let us examine a possible scheme for the process of dissociative ionization on a surface. We assume that after adsorption on the surface is completed the molecules come to thermal equilibrium with the surface, i.e., the temperature of the distribution function of the molecules coincides with the surface temperature  $T$ . The main contribution to the reaction is provided by molecules with a large amount of internal energy, a fraction of which goes into rupturing the dissociable bond.

Thus, if the rate of molecular dissociation is higher than the rate at which they exchange energy with the surface, the equilibrium energy distribution of the molecules is disrupted and a quasi-Maxwellian distribution with the temperature  $T_n < T$  sets in. Initially, the reaction products have the same distribution function with the temperature  $T_n$ , since they had no time to receive energy from the solid and come to equilibrium with it. Now, if the lifetime of the reaction product  $M - H$  at the surface is large, the initial energy distribution relaxes toward a distribution with the temperature of the surface. Raising the probability of ion desorption from the surface by applying an electric field (from the time  $\tau_{i1}$  at which the distribution function has a temperature  $T$  to the

time  $\tau_{in}$  corresponding to the temperature  $T_n$ ), we can trace (by examining the change in the slope of the delays) the way in which the temperature of the distribution function of the reaction products changes from  $T$  to  $T_n$ . Thus, if the scheme we are describing is true, the time variation in the lifetime of ions on the surface, characterized by the quantity  $(\tau_{i1}/\tau_{ii})(F)$ , must be proportional to the change  $\Delta T(F)$  in the temperature of the distribution function of the reaction products.

#### 4.4 The possibility of determining the shape of potential curves characterizing the interaction of polyatomic ions with a surface

Let us see how to determine the interaction potential of a polyatomic particle and a surface by varying the ion-accelerating electric field applied to the surface. The height of the Schottky barrier forming in such a field and the distance  $x_0$  from the top of the barrier to the surface are determined by the strength  $F$  of the applied field [2]. By finding from experiments the desorption energy  $I_F^+$  of the polyatomic ion we can reconstruct (determine) the interaction potential between this particle and the surface as a function of the distance between them, i.e.,  $I_F^+(x_0)$ . Let us represent this function analytically with allowance for the correction  $\delta(F)$  introduced in Ref. [2] (see Section 2.4).

We begin with the Schottky relation [2] at  $F = 0$ :

$$I^0 - I^+ = e(\varphi - V).$$

When an electric field is switched on, the ion desorption heat decreases by  $\Delta\lambda(F) = \lambda_+ - \lambda_+^F = I^+ - I_F^+$  [2], and the level from which the vacuum potential is counted changes by  $eFx_c$  [2]. Thus, the difference  $I^0 - I_F^+$  (for  $F \neq 0$ ) can be written down as follows:

$$I^0 - I_F^+ = I^0 - I^+ + \Delta\lambda(F) = e(\varphi - V) + \Delta\lambda(F) + eFx_c. \quad (34)$$

Next, we introduce correction  $\delta(F)$  [2] into  $\Delta\lambda(F)$  [which is absent in Eqn (15)], which accounts for the work done by the rapidly decreasing polarization and dispersion forces and for the possible deviation in the image potential  $e^2/(4x^2)$  for the ion. Then, at the point  $x_0$  of the balance of forces (where the first derivative of the sum of all potentials acting on the ion vanishes) we have the relationship

$$\frac{e^2}{4x_0^2} - \frac{d\delta(F)}{dx} \Big|_{x_0} = eF(x_0),$$

which allows us to determine the dependence of the position of the point  $x_0$  on the field  $F$ :

$$x_0(F) = \frac{e}{2} \sqrt{\frac{1}{eF + \delta'_x}} \approx \frac{1}{2} \sqrt{\frac{e}{F} \left( 1 - \frac{\delta'_x}{eF} \right)}. \quad (35)$$

The quantity  $\Delta\lambda$  can be found by integrating the forces acting on the ion over the coordinate from the critical distance  $x_c$  to  $x = \infty$  at  $F = 0$ , and to  $x = x_0$  for  $F \neq 0$ :

$$\Delta\lambda(F) = \int_{x_c}^{\infty} \left( \frac{e^2}{4x^2} - \frac{d\delta(0)}{dx} \right) dx - \int_{x_c}^{x_0} \left( \frac{e^2}{4x^2} - \frac{d\delta(F)}{dx} - eF \right) dx.$$

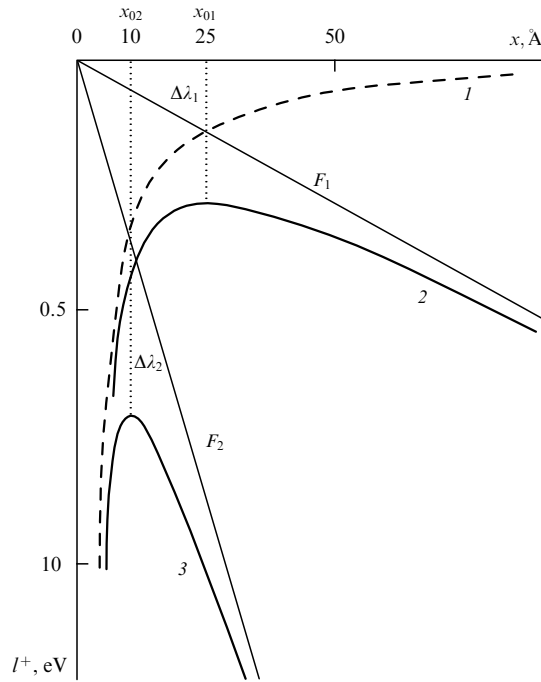


**Figure 3.** Variation in the heat  $I^+(x)$  of ion desorption from a conducting surface at the field strengths  $F_1 = 5.7 \times 10^5 \text{ V cm}^{-1}$  and  $F_2 = 3.4 \times 10^6 \text{ V cm}^{-1}$ . Curve 1 corresponds to the Coulomb interaction between a charge and the conducting surface, while curves 2 and 3 represent the sums of the Coulomb potential and the  $eFx_i$  potentials.

Assuming that  $F = \text{const}$  for  $x \leq x_0$  and that the critical distance  $x_c$  is field-independent, we arrive at

$$\Delta\lambda(F, x) = \frac{e^2}{4x_0} + eFx_0 + \delta(x_0, F) - \delta(x_c, F) + \delta(x_c, 0) - eFx_c. \quad (36)$$

Notice that Eqn (36) at  $\delta(F) = 0$  coincides with Eqn (15).

Equation (36) shows that the contributions  $\delta(F, x)$  can be divided into two groups: the contributions  $\delta(x_c, 0) - \delta(x_c, F)$  caused by the effect of  $F$  on charge exchange at the point  $x_c$ , and the contribution  $\delta(F)$  related to the change in the equilibrium distance  $x_0$  caused by variations in  $F$ . A discussion of the role of these contributions will be held later when analyzing experimental results; here, as before, we denote their sum by  $\delta(F)$ .

For point ions we have  $\delta(F) = 0$ . Combining Eqns (35) and (36) with this case, we arrive at the well-known result (see Ref. [2]): the distance from the surface at which the barrier's height decreases by  $\Delta\lambda(F) = e\sqrt{eF}$  is  $x_0 = (1/2)\sqrt{e/F}$ .

Figure 3 illustrates the proposed method and shows the behavior of  $\lambda(F_1)$  and  $\lambda(F_2)$ , as well as the points  $x_{01}$  and  $x_{02}$  for two values of the field ( $F_1 = 5.7 \times 10^5 \text{ V cm}^{-1}$  and  $F_2 = 3.4 \times 10^6 \text{ V cm}^{-1}$ ). It also displays the Coulomb curve representing the interaction of the ion with a conducting surface in a zero electric field (curve 1).

In the case of dissociative surface ionization in an electric field, the expression for  $\delta(F)$  can be obtained by comparing Eqns (34) and (36) with the equation (5) for the ion current, which can be written out with the all  $F$ -dependent parameters incorporated in the exponent:

$$I^0 - I_F^+ = \Pi - E + \delta = \Pi - E + k_B T b(F) \ln \left( \frac{E}{k_B T} \right). \quad (37)$$

Thus, for the empirical value of  $\delta$  we take

$$\delta(F) = k_B T b(F) \ln \left( \frac{E}{k_B T} \right). \quad (38)$$

Allowing for relationship (38), we can find the explicit form of  $d\delta(F)/dx$  suitable for calculating  $x_0(F)$  in formula (35):

$$\begin{aligned} \frac{d\delta(F)}{dx} &= \frac{d\delta(F)}{dF} \frac{dF}{dx} \\ &\approx -\frac{F}{r} k_B T \ln \left( \frac{E}{k_B T} \right) \frac{db(F)}{dF} = \delta'_x. \end{aligned} \quad (39)$$

The derivative  $dF/dx = -F/r$  was found from a series expansion in powers of  $x/r \ll 1$  of the expression for the field of a cylindrical capacitor with an inner electrode (emitter) of radius  $r$ .

Calculations of  $\delta'_x$  and  $x_0$  involve using the experimental values of  $db/dF$  for ions  $(M-H)^+$  of triethylamine (TEA) and tetramethyldiaminomethane (TMDM) [12].

To determine the values of the potential  $I_F^+(x)$ , we take the difference in expressions (34) for two different values  $F_i$  and  $F_1$  of the electric field. Since the interaction between the radical  $M-H$  and the surface is determined by a strong chemical bond which depends only slightly on the field strength, we ignore (just as we did before) the variations of  $l_0$  as the field strength grows from  $F_1$  to  $F_i$  ( $i = 2, \dots, 5$ ). If  $F_i \gg F_1$  for all  $i$ s, then in setting up the difference  $I_{F_i}^+ - I_{F_1}^+$  we can ignore the terms  $e^2/(4x_{01})$  and  $eF_1 x_{01}$ , whose values are within the experimental error. Then Eqns (34) and (36) yield

$$-(I_{F_i}^+ - I_{F_1}^+) = -\Delta I_i^+ = \frac{e^2}{4x_{0i}} + eF_i x_{0i} + \delta(F_i) - \delta(F_1). \quad (40)$$

Equation (40) describes the behavior of curves of type 2 or 3 in Fig. 3. To describe the behavior of curves of type 1, we must transpose the term with  $eF_i x_{0i}$  to the left-hand side of Eqn (40). Then, with allowance for formula (38) we can write down an expression for the interaction potential  $U(x_0)$  acting between an ion and a conducting surface:

$$U(x_0) = -(\Delta I_i^+ + eF_i x_{0i}) = \frac{e^2}{4x_{0i}} + k_B T \ln \left( \frac{E}{k_B T} \right) \Delta b(F_i), \quad (41)$$

where  $x_0$  can be found from Eqn (35).

We see from the last relationship that the deviation in the interaction potential of polyatomic ions from the Coulomb interaction potential of point charges is proportional to quantities determined from experiments, including  $\Delta b$ . The same quantity determines in Eqn (26) the difference between the field dependences of the currents of polyatomic and monatomic ions (see Section 5.1, Fig. 5).

#### 4.5 Photodesorption field IR spectroscopy

In the method under discussion, the adsorbed molecules are excited by monochromatic infrared (IR) radiation within the range of their natural vibrations. The excited particles are ionized by nonequilibrium surface ionization in a strong electric field ( $\tau_i < \tau_r$ ), which leads to an increase in the ionization efficiency (18). Thus, what is new in the proposed method is that it established a relation between the current of ions desorbing from the surface (in the presence of a strong electric field) and the varying frequency of the IR radiation

incident on this surface. Since the method relies on mass-spectrometric studies, we need to keep track of the current generated by ions of a certain mass, the current being increased only if the incident radiation excites in adsorbed molecules or their fragments precisely those vibrations that lead to the desorption of ions of these particles. Thus, the recorded spectrum (i.e., the dependence of the ion current on the radiation frequency) is the desorption vibrational spectrum of the adsorbed molecules and their fragments.

All additions to the device necessary for irradiating the emitter of ions by a flux of electromagnetic radiation are rather simple and must meet a few obvious conditions.

When IR radiation is utilized, the optimum angle of incidence of light on a flat emitter amounts to  $88^\circ$  [36]. When the emitter is a cylinder, it is important that the value of this angle fits into the collection angle for the ions being desorbed from the surface, i.e., fits into the aperture of the mass spectrometer. Thus, a cylindrical emitter can be illuminated at a right angle to the electron-optical axis of the source, since the collection angle of the ion beam in the field source is  $\pm 3^\circ$ . Sapphire windows were employed to let in the IR radiation, and they were located at right angles to the electron-optical axis of the field source of ions. For the source of IR radiation we took an incandescent SIRSh-200 lamp which illuminated the entrance slit of an MDR-23 monochromator (the monochromator was part of a spectral computer KSVU-23 complex). Variations in the ion current  $j$  at the exit slot of the mass spectrometer were recorded by the computer entering the KSVU complex onto the vertical axis of the  $j$  vs.  $\lambda$  dependence. The recording of the spectrum  $j(\lambda)$  was done by sweeping the wavelength  $\lambda$  along the horizontal axis within the 1600–2000-nm and 2000–3000-nm ranges with a 20-nm increment.

#### 4.6 The possibility of estimating the absorption of IR radiation by adsorbed molecules

Let us derive an expression for the variation in the ion current produced by nonequilibrium surface ionization ( $\alpha \ll 1$ ) when IR radiation is absorbed by adsorbed molecules, an expression that can be used for estimating the absorption cross section  $\sigma$  of such radiation by adsorbed molecules.

The flux  $g$  which determines the concentration  $n^*$  of particles on a surface is related to  $n^*$  through the lifetimes of the neutral and ionic components [2]:

$$g = n^* \left( \frac{1}{\tau_i} + \frac{1}{\tau^0} \right).$$

When there is a strong electric field, we have  $\tau_i \ll \tau^0$ , with the result that

$$g = \frac{n^*}{\tau_i}.$$

When the surface is illuminated, some of the adsorbed molecules go into a vibrationally excited state and are desorbed in the form of ions whose current is determined by the degree  $\alpha_n$  of nonequilibrium surface ionization:

$$\Delta j \approx e \Delta g \alpha_n = e \Delta g A_n \exp \frac{\Pi}{k_B T_n},$$

where  $A_n$  is the ratio of the partition functions of the ionic and neutral states of a particle, and the population of these states is governed by the nonequilibrium temperature  $T_n$ .

The magnitude of the flux  $\Delta g$  of excited particles is proportional to the concentration of the particles, the intensity  $I$  of the radiation, and the radiation absorption cross section  $\sigma$ :

$$\Delta g = n^* I \sigma,$$

where  $I = P/Shv$ , with  $h\nu$  being the photon energy,  $P$  the radiation power, and  $S$  the area of the illuminated surface that fits into the aperture of the mass spectrometer [37].

Then the ratio of  $\Delta j$  to the equilibrium current  $j$  (background current without illumination of the emitter) can be written down as follows:

$$\frac{\Delta j}{j} = \frac{\Delta g}{g} \frac{\alpha_n}{\alpha} = I \sigma \tau_i \exp \left[ \frac{\Pi}{k_B T_n} \left( -\frac{\Delta T}{T} \right) \right]. \quad (42)$$

The ratio  $A_n/A$  is close to unity, since the following inequalities  $h\nu > k_B T_n > k_B T$  are met. We also note that relationship (42) contains  $\tau_i$ , since a nonequilibrium current can be observed only if  $\tau_i < \tau_r$  [see Eqn (2)].

## 5. Experiments and a discussion

### 5.1 Determining the parameters of dissociative surface ionization of polyatomic molecules

As objects for studying dissociative ionization in an electric field at the surface of pure tungsten, we selected (see Refs [12, 13, 28]) substances with the lowest values of the ionization potentials of the  $M-H$  radicals, studied by Zandberg et al. [30, 38]. The ionization potential of the  $M-H$  radicals of triethylamine (TEA) amounts to 6.9 eV, and that of tetramethyldiaminomethane (TMDM) to 6.1–6.5 eV [4]. Their structural formulas are depicted in Fig. 4. The temperature of the filament in our experiments, determined by an optical micropycrometer, was varied from 1000 to 2000 K. The work function was determined from the function  $j(T)$  for indium atoms. The pressure of residual gases was about  $10^{-9}$  Torr, while the pressure of the investigated gas was maintained at a level of  $2 \times 10^{-7}$  Torr.

The separation of ions in mass spectrometers is done according to the parameter  $m/e$ , where  $m$  is the ion mass, and  $e$  is the elementary charge. For singly charged ions, the position of the ion peaks on the  $m/e$ -axis corresponds to their position on the (mass)  $m$ -axis in atomic mass units (a.m.u.). Only singly charged ions are produced with surface-ionization sources.

In the TEA mass spectrum we observed, just as Zandberg and Rasulev [38] did,  $(M-H)^+$  ions with a mass of 100 a.m.u. and  $(M-CH_3)^+$  ions with a mass of 86 a.m.u. The current intensity of  $(M-CH_3)^+$  ions amounted to no more than 1% of the main peak in the current intensity of  $(M-H)^+$  ions. The spectrum also revealed the presence of ions with masses

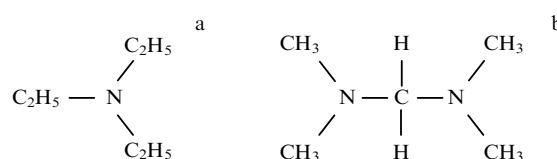


**Figure 4.** Structural formulas of (a) triethylamine (TEA), and (b) tetramethyldiaminomethane (TMDM).

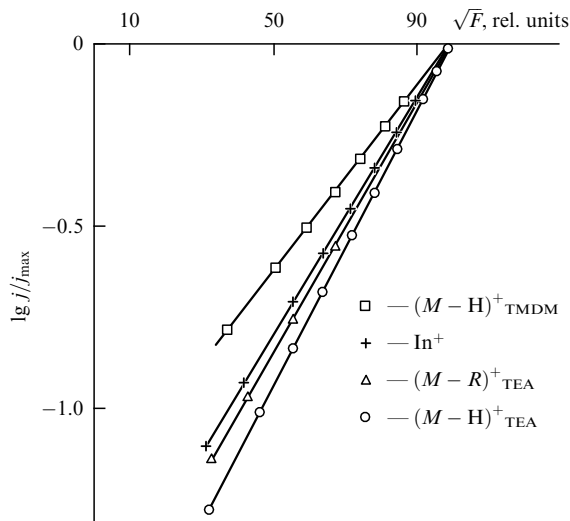
amounting to 72 and 51.8 a.m.u., which were produced as a result of disintegration of the metastable  $(M-H)^+$  ions on their way from the emitter to the boundary of the mass-spectrometer magnetic field and having a current intensity that is lower than that of  $(M-H)^+$  ions by a factor of 100. Such a relationship between the peak intensities of the above-mentioned ions suggests that the reaction  $M \rightarrow (M-H) + H$  is a single-channel one.

In our experiments we studied the dependences  $j(F)$  at  $T = \text{const}$ ,  $j(T)$  at  $F_k = \text{const}$ ,  $k = 1, \dots, 5$ , and  $j(U_d)$  at  $T = \text{const}$  and  $F_n = \text{const}$ ,  $n = 1, \dots, 10$  for constant fluxes of TEA molecules and In and Cs atoms (simultaneous inflow) onto the surface. For all variations in  $F$  for  $M-H$ ,  $M-R$ , and In we always held the inequality  $e(V - \phi - \sqrt{eF}) \gg k_B T$ , i.e.,  $\alpha \ll 1$ .

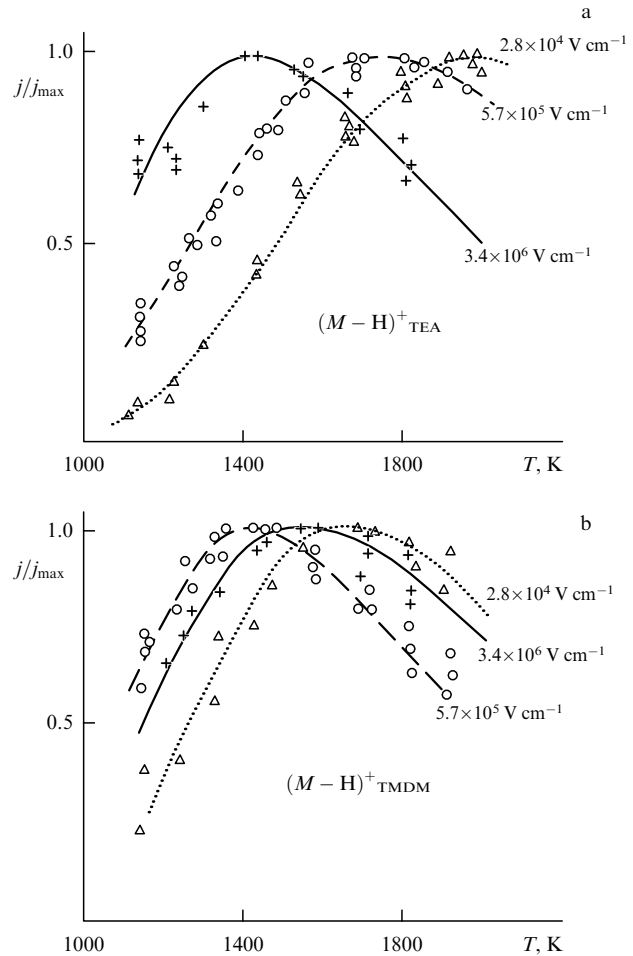
Figure 5 shows the dependences  $\lg j/j_{\max} = f(\sqrt{F})$  for the currents of the ions  $\text{In}^+$ ,  $(M-H)^+$ , and  $(M-CH_3)^+$  of TEA and  $(M-H)^+$  of TMDM. The experimental points obtained with the fields ranging from  $2 \times 10^5$  to  $3 \times 10^6 \text{ V cm}^{-1}$  were approximated by straight lines. The temperatures  $T_F$ , determined from the slopes of the curves using Eqn (26), proved to be different for the  $(M-H)^+$  and  $(M-CH_3)^+$  ions of TEA and lower than those for  $\text{In}^+$ . The temperature  $T_F$  determined from the plots for  $\text{In}^+$  ions coincides with the filament's pyrometric temperature. The temperatures  $T_F$  for fragmented ions with masses  $m$  amounting to 51.8 and 72 a.m.u. coincided with the temperature  $T_F$  of the parent  $(M-H)^+$  ions.

Figure 6a displays the ratios  $j/j_{\max}$  of the currents of  $(M-H)^+$  ions as functions of the filament temperature  $T$  for three values of  $F$ . As  $T$  increases, the functions pass through their maxima and shift toward lower temperatures as  $F$  grows [see Eqn (21)], with the half-width of the curves decreasing in the process [see Eqn (23)].

Figure 7 presents the initial straight-line segments of the delay curves for  $\text{Cs}^+$ ,  $(M-H)^+$  of TEA, and  $(M-H)^+$  of



**Figure 5.** Dependences of  $\lg(j/j_{\max})$  as functions of  $\sqrt{F}$  for the dissociative ions  $(M-H)^+$  and  $(M-R)^+$  of the molecules  $(M)$  of triethylamine (TEA) and tetramethyldiaminomethane (TMDM) and for indium atomic ions under surface ionization on tungsten at  $T = 1800 \text{ K}$  (H stands for a hydrogen atom, and R is a radical). Here,  $j_{\max}$  is the ion current with the field  $F$  at its maximum value in the experiment. The slopes of the graphs correspond to the field temperature  $T_F$ , which for  $\text{In}^+$  ions coincides with the surface temperature. Only for  $(M-H)^+$  ions of TMDM was the temperature  $T_F$  found to be higher than the surface temperature.



**Figure 6.** The temperature curves of the reduced currents  $(j/j_{\max})(T)$  of  $(M-H)^+$  ions of TEA (a), and of  $(M-H)^+$  ions of TMDM (b) at  $T = 1800 \text{ K}$  and different values of the field strength (indicated in the figure) for surface ionization on tungsten. The value  $j_{\max}$  corresponds to the maximum ion current. The experimental data are indicated by various symbols. Dotted, dashed, and solid curves represent the calculated temperature curves for the indicated field strengths [12]. As the field strength  $F$  grows, the bell-shaped temperature curves for the  $(M-H)^+$  ions of TEA shift toward lower temperatures with the half-width of the curve decreasing in the process. For  $F > 10^6 \text{ V cm}^{-1}$ , the temperature curves for the  $(M-H)^+$  ions of TMDM shift, as the field strength increases, toward higher temperatures, with the half-width of the curve increasing in the process.

TMDM. The slope of the graph  $\lg j/j_{\max} = f(U_d)$  for  $\text{Cs}^+$  ions corresponds, to within the instrumental factor, to the emitter temperature. The slope of the graph for  $(M-H)^+$  ions of TEA yields a temperature that is lower than the emitter temperature by  $130 \pm 30 \text{ K}$ . The delay curves were measured at  $F = 1.65 \times 10^6 \text{ V cm}^{-1}$  and  $T = 1800 \text{ K}$ .

In our studies of surface ionization of TMDM molecules (see Ref. [12]), the mass spectrum revealed (just as it did in the study by Zandberg et al. [30]) the presence of  $(M-H)^+$  ions with  $m = 101 \text{ a.m.u.}$  and  $(M-R)^+$  ions with  $m = 58 \text{ a.m.u.}$  The current intensity of  $(M-R)^+$  ions amounted to roughly 10% of the intensity of the main peak of the current of  $(M-H)^+$  ions. The mass spectrum also revealed the presence of metastable ions with masses  $m = 86$  and  $73.2 \text{ a.m.u.}$ , whose current intensity did not exceed 0.2–0.4% of that of the initial  $(M-H)^+$  ions. For  $(M-H)^+$  and  $(M-R)^+$  ions, the condition  $\alpha \ll 1$  was met. The graph  $\lg j/j_{\max} = f(\sqrt{F})$  (see

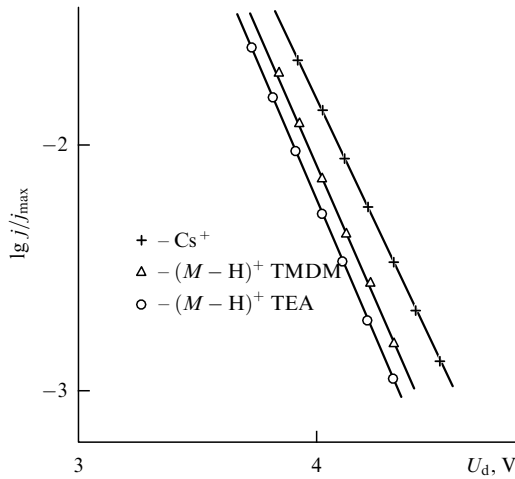


**Figure 7.** Straight-line segments of the delay curves  $\lg(j/j_{\max})(U_d)$  (here,  $j_{\max}$  is the saturation current as  $U_d \rightarrow 0$ ) for  $(M-H)^+$  ions of TEA,  $(M-H)^+$  ions of TMDM, and  $Cs^+$  ions produced by surface ionization on tungsten at  $T = 1800$  K and  $F = 1.7 \times 10^6$  V cm $^{-1}$ . The temperature ( $T_d$ ) of the  $Cs^+$  ions, determined from the graph's slope, is equal to the surface temperature.

Fig. 5) displays that the temperature  $T_F$  (determined from the slope) for  $(M-H)^+$  ions of TMDM is higher than that for  $In^+$ . [In the case of  $(M-R)^+$  ions, not shown in the figure,  $T_F$  is lower than that for  $In^+$ .] The temperature  $T_F$  for the metastable ion with  $m = 86$  a.m.u. was found to coincide with the temperature for the parent  $(M-H)^+$  ion.

As  $T$  increases, the curves representing the dependence  $j(T)$  for  $(M-H)^+$  ions (Fig. 6b) pass through their maxima and shift toward lower temperatures as the field strength increases to  $F \sim 2 \times 10^6$  V cm $^{-1}$ , but then shift toward higher temperatures as the field strength increases still further. When the curves shift toward lower temperatures, their half-widths decrease, but they increase when the curves shift toward higher temperatures.

The initial straight-line segments of the delay curves for  $(M-H)^+$  ions of TMDM molecules yield a temperature  $T_d$  that is lower than the emitter temperature by  $120 \pm 30$  K (just as in the case of TEA). The delay curves were measured at  $F = 1.65 \times 10^6$  V cm $^{-1}$  and  $T = 1800$  K (see Fig. 7).

Thus, the temperatures corresponding to the distribution of ions over their normal velocities of translational motion at  $F = 1.65 \times 10^6$  V cm $^{-1}$  for  $(M-H)^+$  of TEA and TMDM proved to be lower than the emitter temperature. At such field strengths, the lifetime of ions at the surface diminishes by a factor of approximately 10, with the result that the ion distribution functions characterize the initial stages of the reaction, which, as noted earlier, are described by nonequilibrium distribution functions. The fact that the distribution functions show departure from equilibrium ones in dissociation reactions reflects a situation in which the particles with the highest energies enter into the reaction, as a result of which the ion energy distribution function is enriched in slow particles, and this leads to a lowering of the temperature of the distribution function in high electric fields.

The relaxation of the distribution functions of  $(M-H)^+$  ions of TEA was studied in experiments in which the field strength ranged from  $5 \times 10^4$  to  $4 \times 10^6$  V cm $^{-1}$ . The characteristic features of the curves in Fig. 8 in the vicinity of  $F^* = 2 \times 10^6$  V cm $^{-1}$ , the difference in the field tempera-

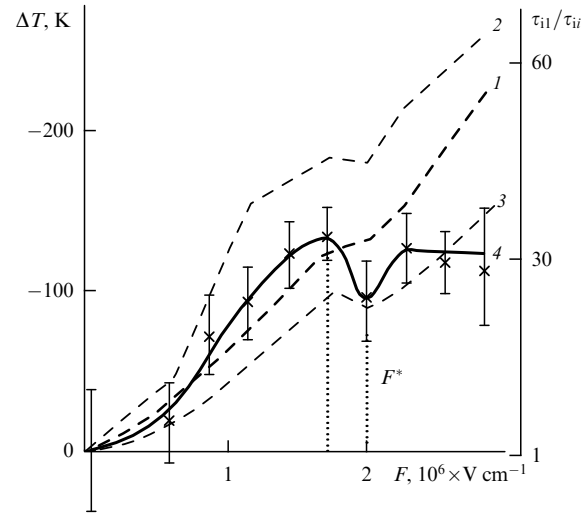


**Figure 8.** Dependences of the relative lifetime  $\tau_{ii}/\tau_i$  of  $(M-H)^+$  ions of TEA molecules on the field strength  $F$  (the right vertical axis, curves 1–3) in surface ionization on tungsten ( $T = 1800$  K). Curve 1 represents the average values of  $\tau_{ii}/\tau_i$ , curves 2 and 3 were obtained under variations in  $E$  and  $\Delta b$  within experimental errors, and curve 4 depicts the dependence of the temperature difference  $\Delta T = T_d[(M-H)^+TEA] - T_d(Cs^+)$  on the field strength  $F$  (the left vertical axis). The temperatures  $T_d[(M-H)^+TEA]$  and  $T_d(Cs^+)$ , which characterize the energy distribution functions of these ions, were obtained from the slopes of the curves  $j(U_d)$  by the retarding potential method. The value of  $\Delta T_n$  corresponding to the point where the curve flattens out and characterizing the magnitude of the dissociation reaction departure from equilibrium is equal to  $\Delta T_n = -35 \pm 15$  K, with allowance for the correction for the dependence on pressure (the graph yields  $\Delta T \sim -120$  K).

tures  $T_F$  of the  $(M-H)^+$  ions of TEA and TMDM molecules, and peculiarities of the shift in  $j(T)$  related to the variation in  $F$  can be attributed to the shape of the potential curves characterizing the ion–surface interaction, which will be discussed in Sections 5.5 and 5.6.

Using the obtained experimental data in formulas (21), (24), and (28), we found the following values of the parameters: for the  $M-H$  radical of TEA, the number  $b$  of degrees of freedom varied, as  $F$  increased from  $10^5$  to  $3.4 \times 10^6$  V cm $^{-1}$ , within the limits  $b = (12 - 14 - 12) \pm 1$ ; the ionization potential  $eV_{TEA}$  of the  $M-H$  radical amounted to  $6.9 \pm 0.1$  eV; the dissociation activation energy  $E$  for  $M$  molecules at the surface was  $0.2 \pm 0.05$  eV, while for  $M-H$  of TMDM the analogous parameters were  $b = (16 - 14 - 11) \pm 1$ ,  $E = 0.2 \pm 0.05$  eV, and  $eV_{TMDM} = 6.8 \pm 0.1$  eV.

Let us compare the last result with the estimates given by Zandberg et al. [4, 30] for the ionization potentials of the  $M-H$  radicals of TMDM, which amount to  $eV \leq 6.5$  eV for ionization on wires, and to  $eV \leq 6.1$  eV for ionization on ribbons. In our experiments, the value of the ratio of the currents of the  $M-H$  radicals of TMDM and TEA,  $j_{TMDM}/j_{TEA}$ , was roughly 10. Allowing for formula (5), we can write out this ratio in the following form:

$$\frac{j_{TMDM}}{j_{TEA}} = \left( \frac{E}{k_B T} \right)^{b_{TMDM} - b_{TEA}} \exp \frac{eV_{TEA} - eV_{TMDM}}{k_B T},$$

since the activation energy  $E$  needed for the formation of an  $M-H$  radical is the same for both molecules. The value of the ratio  $j_{TMDM}/j_{TEA}$  calculated by this formula with  $eV_{TMDM} = 6.5$  eV and  $T = 1500$  K amounted to roughly 120, while with  $eV_{TMDM} = 6.8$  eV it became equal to roughly

12, agreeing better with the measured ratio of currents. Hence, we assume that the ionization potential of the  $M-H$  radical of TMDM, or  $eV_{TMDM}$ , is  $6.8 \pm 0.1$  eV.

### 5.2 Relaxation of the energy distribution functions of products of dissociative surface ionization

Measurements of the delay temperatures  $T_d(M-H)^+$ , which characterize the temperatures of the distribution function of the  $(M-H)^+$  ion of TEA, were done at different field strengths  $F$  at strictly constant TEA pressure, since the value of  $T_d(M-H)^+$  depends on the TEA pressure in the chamber. The dependence of  $\Delta T$  on the TEA pressure  $P$  was considered a systematic error, which was excluded by extrapolating  $\Delta T_d(P)$  to zero pressure in order to obtain the true value of  $\Delta T$ .

As noted earlier (see Fig. 7), the values of  $T_d[(M-H)^+]$  proved to be smaller than those of  $T_d(Cs^+)$ , with  $\Delta T = T_d[(M-H)^+] - T_d(Cs^+)$  depending on the strength of the applied field. In Fig. 8, the values of  $\Delta T$  (prior to extrapolating in pressure) are laid aside on the left vertical axis. The experimental values of  $\Delta T$  are marked by crosses, and the error  $\sigma^*(\Delta T)$  is indicated by vertical bars (the value of  $\sigma^*$  corresponds to a confidence level of 0.9).

Figure 8 also demonstrates the functions  $(\tau_{i1}/\tau_{ii})(F)$  calculated by formula (33) for the  $(M-H)^+$  ions of TEA [39]. Curve 1 represents the average values of  $E$  and  $\Delta b$ , while curves 2 and 3 show the same function with  $E$  and  $\Delta b$  varying within the experimental errors  $(\Delta b, E + \sigma_1)$  and  $(\Delta b - \sigma_2, E)$ , respectively [12, 28]. What is interesting in Fig. 8 is the singularity near  $F^* = 2 \times 10^6$  V cm $^{-1}$ . At this point there is an inflection in curve 1, while curves 2 and 3 have local minima of  $(\tau_{i1}/\tau_{ii})(F)$ . The fact that curves 2 and 3 correlate with curve 4 suggests that the local increase in  $\Delta T$  (from  $\Delta T \approx -130^\circ\text{C}$  to  $\Delta T \approx -90^\circ\text{C}$ ) at the point  $F = F^*$  is related to a decrease in the probability of ion desorption from the surface.

### 5.3 Magnitude of departure from equilibrium in endothermic reactions on a surface

Differences in the behavior of the experimental curves representing  $\Delta T(F)$  and the theoretical curves representing  $(\tau_{i1}/\tau_{ii})(F)$  have been observed beginning with  $F = 2.3 \times 10^6$  V cm $^{-1}$ . The calculated curve continues to rise since, with the exception of point  $F^*$ , the probability of ion emission increases as  $F$  grows, while the experimental points of the  $\Delta T$  values reach a plateau. This suggests that in the event of saturation the measured temperature is  $T_n$ , namely, the temperature of the distribution function of the ions in the initial stages of the reaction, since after that (in the absence of the electric field) the ions begin to exchange energy with the surface and the difference  $\Delta T$  diminishes. By increasing the field strength we can reduce the ion lifetime to such an extent that the ion leaves the surface without exchange energy with the surface, carrying away the initial nonequilibrium value  $T_n$ . Thus, the value  $\Delta T_n = T_n - T$  can be considered the magnitude of departure from equilibrium in the catalytic endothermic reaction of dissociation. With allowance for the pressure correction [39], one finds  $\Delta T_n \approx -35 \pm 15$  K.

### 5.4 Times of energy exchange between reaction products and the surface

The value of  $(\tau_{i1}/\tau_{ii})(F)$ , corresponding to the point where the  $\Delta T$  curve flattens out, gives an idea of the time it takes to

exchange energy between a particle and the surface, or the time during which an equilibrium distribution for a given ion on the surface of a solid sets in. Assuming that on the whole  $\Delta T(F)$  varies according to an exponential law, we define this time interval  $\Delta\tau$  as the time in which a temperature difference that is  $e$  times smaller than the temperature difference  $\Delta T_n$  in the steady state is reached, i.e.,  $\Delta T_e = \Delta T_n [1 - (1/e)]$ . Figure 8 shows that  $\Delta T_n$  corresponds to  $\tau_{i1}/\tau_{in} = 32$ , and that  $\Delta T_e$  corresponds to  $\tau_{i1}/\tau_{i2} = 12$ . The difference in these two values yields the relaxation time  $\Delta\tau$  (the time in which the steady state sets in):  $\Delta\tau = \tau_{i2} - \tau_{in} \sim 5 \times 10^{-2} \tau_{i1}$ , where  $\tau_{i1}$  is the average lifetime of the  $(M-H)^+$  ions on the surface. If in estimating the order of magnitude of  $\tau_{i1}$  we use the values of the desorption heat  $I^+ = 1.2 \pm 0.2$  eV and of the pre-exponential factor  $\lg C = 10.2 \pm 0.9$  [see Eqn (32)], obtained by Zandberg et al. [4, 40] for the  $(M-H)$  radical of the TEA molecule on oxidized tungsten, we obtain  $\Delta\tau_i \sim 10^{-8} - 10^{-9}$  s.

### 5.5 Interaction potentials between polyatomic ions and the surface

Figure 9 depicts the potential curves  $U(x_0)$  for the  $(M-H)^+$  ions of TEA and TMDM molecules obtained by calculating the right-hand side of Eqn (41) on the basis of our experimental data on  $\Delta b(F)$ ,  $E$  and  $db/dF$  [12] and the values of  $x_{0i}$  from Eqn (35), corresponding to these data. The solid part of curve 1 in Fig. 9 is drawn through the experimental points for the  $(M-H)^+$  ion of TEA. The dashed part of curve 1 represents the Coulomb interaction potential of a charge and a conducting surface. The experimental points in the solid part of the potential curve exhibit that there is a descent in the curve in the interval of  $x$  values from 8 to 25 Å. The standard deviation was calculated using the error-transfer formula [41] for  $\Delta\delta(F_i)$ . The variances of the quantities entering  $\Delta\delta(F_i)$  were taken from the experimental data [12].

The presence of an inflection in curve 1 can be explained by the short-range interaction of the  $(M-H)^+$  ion of TEA and a conducting surface, which manifests itself, of course, in addition to the ion-surface Coulomb interaction. Usually,

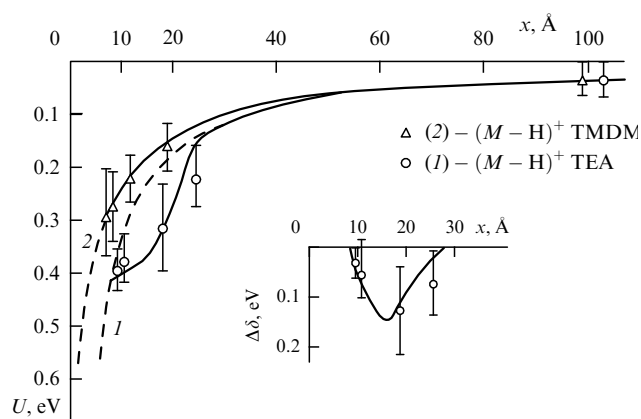


**Figure 9.** The potential curves  $U(x)$  specifying the interaction of polyatomic  $(M-H)^+$  ions of TEA (the solid part of curve 1) and  $(M-H)^+$  ions of TMDM (the solid part of curve 2) with the surface of a metal. The dashed part of curve 1 represents the Coulomb interaction potential of a charge and a conducting surface. The inset shows the curve representing the polarization interaction of a polyatomic ion and a conducting surface, with  $\Delta\delta$  being the difference in the values on the potential curve of the  $(M-H)^+$  ion of TEA (solid part of curve 1) and the Coulomb potential (dashed part of curve 1).



the potential curves of intermolecular interaction are described fairly well by the Lennard–Jones (12–6) potential [42]. According to this model, the coordinate of the point at which the potential curve intersects the horizontal axis is equal to the diameter of the molecule, while the depth of the well amounts to several kilocalories per mole. Although for a polyatomic molecule the idea of the diameter of a molecule is purely a matter of convention, the diameter of a TEA molecule can be estimated at 10 Å.

In the inset to Fig. 9 we have depicted, for the sake of making the comparison with the model potential more pictorial, the difference between the experimental points and the Coulomb curve (the dashed portion of curve 1). The curve representing  $\Delta\delta(x)$  is the potential curve of the polarization interaction between the polyatomic ion and the conducting surface.

Curve 2 in Fig. 9 is a Coulomb curve shifted horizontally by a distance  $x = 7$  Å in relation to curve 1. Clearly, it passes through the experimental points for the  $(M-H)^+$  ion of TMDM. In our opinion, the reason for this is that the TMDM molecule contains two nitrogen atoms. As is known, in the adsorption of amines an electron pair in a nitrogen atom is pulled back toward the emitter, with a consequent formation of a positive charge on the nitrogen atom [4]. When a TMDM molecule is adsorbed, the second nitrogen atom is located at a distance of 3 to 7 Å from the surface. In surface-ionization studies, an electric field of the strength  $F \sim 10^5$  V cm<sup>-1</sup>, which draws off the ions (it is called the drawing field), is always applied across the emitter. Such a field strength is sufficient for the positive charge of the nitrogen ion closest to the surface to move to another nitrogen atom, i.e., the charge in the adsorbed molecule is located farthest from the surface. For this reason, the potential specifying the interaction of an  $(M-H)^+$  ion of TMDM (curve 2) with the surface is lower than in the case of an  $(M-H)^+$  ion of TEA, which explains the essentially lower energy of desorption activation for an  $(M-H)^+$  ion of TMDM (about 1 eV) compared to the desorption activation energy of similar ions of various amines [40]. What is interesting is that the temperature  $T_F$  of the  $(M-R)^+$  ion of TMDM, which contains one nitrogen atom (formed by the rupture of one of the CH<sub>2</sub>–N bonds), is lower than the surface temperature (which is true of other organic ions as well), in contrast to the temperature  $T_F$  of the  $(M-H)^+$  ion of TMDM, which is higher than  $T$ .

Since the  $(M-H)^+$  ion of TMDM, entangled in desorption, is oriented primarily along the field vector down the N–C–N bond, i.e., along its length (whose ratio to the ‘width’ of the ion is roughly 2:1), the dispersive interaction with the surface is weakened [42] and, possibly, is not revealed in the potential curve for the  $(M-H)^+$  ion of TMDM.

### 5.6 A physically adsorbed state of polyatomic ions near a metal surface in an electric field accelerating ions

Figure 10 demonstrates the potential curve of the  $(M-H)^+$  ion of TEA with two inflections: at  $x \approx 25$  Å, and at  $x \approx 9$  Å. Graphically adding this potential curve with two inflections and the field’s potential  $x F_i$  produces a set of curves with two maxima located at a distance of 9 and 25 Å from the surface. At a certain value  $F^*$  of the field strength, the heights of the first and second maxima become equal, i.e., conditions are created for the ion to reside in a physically adsorbed state. Indeed, if  $F > F^*$ , the height of the second maximum (at 25 Å) is smaller than that of the first (at 9 Å), with the result

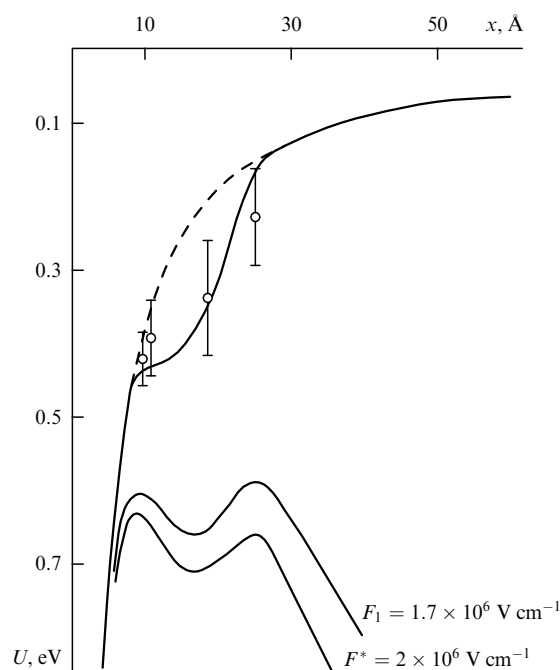


**Figure 10.** A portion of the potential curve  $U(x)$  of the  $(M-H)^+$  ion of TEA (see Fig. 9). In the lower part of the figure, the same potential curve is shown for two different values of  $F_i$ . When  $F^* < F < F_1$ , conditions are created for the existence of the polyatomic  $(M-H)^+$  ion of TEA in a physically adsorbed state (when the two potential barriers have the same heights).

that the moving ion should lose a substantial amount of energy if it ‘wants’ to stay in the well. If  $F < F^*$ , the situation is just the opposite, with the result that the ion bounces from the second maximum, which in either case reduces the probability of the ion residing in the physically adsorbed state.

The  $(M-H)^+$  ions of TEA have no unpaired electrons, which makes them similar to molecules for which it is known (see Ref. [2]) that if the potential curve representing their interaction with the surface exhibits a minimum determined by the van der Waals interaction, they can be in a physically adsorbed state.

Let us consider a situation in which particles that leave the surface are those that are not fully accommodated due to their short lifetime at the surface. Then the lifetime (at the surface) of polyatomic ions landing in the physically adsorbed state increases and, hence, they can receive additional energy from the surface, i.e., the temperature of their distribution function increases. Thus, the curve representing  $\Delta T(F)$ , which characterizes the distribution function of polyatomic ions in relation to the field strength, will have a maximum at a certain value  $F^*$  of the field strength. Figure 10 exhibits that at a certain value of the field strength falling within the interval between the experimental values  $F_1 = 1.7 \times 10^6$  V cm<sup>-1</sup> (upper curve) and  $F^* = 2 \times 10^6$  V cm<sup>-1</sup> (lower curve), the maxima of the curve  $U(F)$  even out. Remaining within the limits of the errors of  $U(F)$  and the size of the field’s increment ( $0.3 \times 10^6$  V cm<sup>-1</sup>), we can assume that the magnitude of this field is  $F^* = (2.0 \pm 0.2) \times 10^6$  V cm<sup>-1</sup> (see Fig. 8) and that in such a field there is a local increase in  $\Delta T$  (from  $\Delta T \approx -130^\circ\text{C}$  to  $\Delta T \approx -90^\circ\text{C}$ ) in the dependence  $\Delta T(F)$  of the temperature of the distribution function of  $(M-H)^+$  ions of TEA on the field strength.

Thus, the presence of a physically adsorbed state for polyatomic ions near a metal surface in an accelerating electric field is confirmed by both the shape of the interaction potentials between the polyatomic ions and the conducting surface (see Fig. 10) and by the presence of a singularity in the dependence of the temperature of the distribution function of these ions on the field strength (see Fig. 8).

This fact, together with the shift in the potential curve of the  $(M-H)^+$  ion of TMDM toward lower energies of interaction with the surface, corroborated by independent measurements [40] of the low desorption activation energy for this ion, indicates that there is a contribution  $\delta(x_0, F)$  brought about by the deviation of  $x_0(F)$  from the Coulomb curve [see Eqn (35)] to the deviation effect in the potential curves for polyatomic ions from the Coulomb curves, in addition to the possible electric field effect on the adsorbed molecule [the term  $[\delta(x_c, 0) - \delta(x_c, F)]$  in Eqn (36)] (the Stark effect and/or a change in the molecule conformation in response to the electric field).

### 5.7 Determining the parameters of surface multimolecular complexes

We now examine the temperature dependence of the current for the associative ion  $(M+H)^+$  of ethylamine [4], shown in Fig. 11 and described, in principle, by Eqn (6). Using the known values  $T_1$  and  $T_{\max}$ , we find from formula (29) that  $b^* = 118$  and  $b^*k_B T_{\max} = 5.85$  eV. The number  $n$  of atoms in the ethylamine molecule  $C_2H_5NH_2$  is 10, so that  $s = 3n - 6 = 24$  and  $b = 6 - 8$ . The ionization potential  $eV$  of ethylamine is 7.8 eV, the work function  $e\phi$  of the surface (oxidized tungsten) is 6.5–6.8 eV, and the dissociation activation energy  $E = 0.2$  eV [12]. Using these data and Eqn (28) we can determine  $E_N$ , whose average value amounts to roughly 0.65 eV, while formula (29) can be employed to find the average number of molecules,  $N = 13 \pm 1$ , for the multimolecular complex of ethylamine molecules.

Let us now examine the temperature dependence of the current for the associative ion  $(M+H)^+$  of diethylamine (DEA) [4], also shown in Fig. 11. For this case,  $b^* = 217$ , and  $b^*k_B T_{\max} = 10.85$  eV. The number  $n$  of atoms in the diethylamine molecule  $(C_2H_5)_2NH$  is 16, so that  $s = 42$ ,  $b = 13 - 18$  (because of the very large value of  $b^*$  we assumed that the number of active degrees of freedom of the given molecule exceeds the value established by the empirical rule), and  $eV = 7.2$  eV. Then, for  $E_N$  we have the average value of

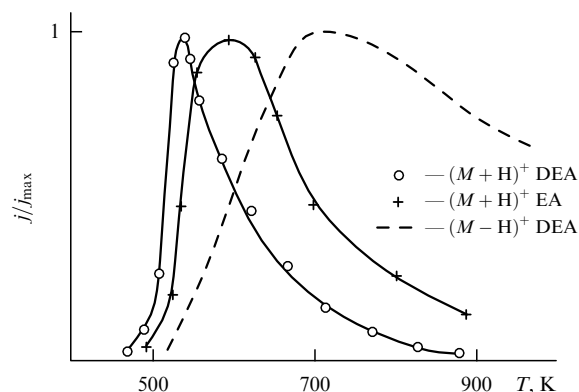


**Figure 11.** Temperature curves of the relative current  $j/j_{\max}$  of  $(M+H)^+$  ions of diethylamine (DEA) and ethylamine (EA) in surface ionization on oxidized tungsten. (According to the data of Ref. [4].)

0.8 eV, while  $N = 14 \pm 2$ . The magnitude of error in  $N$  is determined by a spread of  $b$ .

It is interesting to note that while  $b^*$  values are so different in these two cases, the number of molecules comprising the multimolecular complex is roughly the same and equal to the hexagonal packing factor  $6n + 1$  with  $n = 2$  (here,  $n = 1, 2, \dots$ ) [43].

The reader will recall that, as shown in Section 2 (see also Ref. [11]), the extraction of the associate  $M + H$  from the multimolecular complex in the process of the complex's monomolecular disintegration is a second-order reaction. The order of the reaction, determined in experiments involving associative ions, conducted by Zandberg and Rasulev [4, 32], also proved to be equal to two.

### 5.8 Ionization of energy-saturated compounds on a surface — nonequilibrium surface ionization

We investigated (see Refs [6, 9]) the heterogeneous disintegration of trimeric acetone peroxide (TAP),  $(CH_3)_6(O_2)_3C_3$ , whose structural formula is illustrated in Fig. 12. When explosives disintegrate, electronically excited states of the disintegration products (light flash) and vibrationally excited states of the products (expansion of substance) are observed. In the process of TAP disintegration, ions with a temperature of the distribution functions that exceeded the surface temperature of 1200 K by 500–800 K were registered [6, 31]. Thermal TAP disintegration was found to lead chiefly to the formation of oxygen-containing molecules and radicals, whose ionization potentials were on the average in the 9–11-eV range. In ordinary conditions and even at electric field strengths of  $F = 10^6$  V cm $^{-1}$  near the emitter, substances with such potentials cannot be ionized at a surface. Hence, when there is an ion current, ionizing background substances with the same values of ion mass but with lower ionization potentials becomes a pressing problem. For instance, at  $m = 58$  a.m.u. we can expect a molecular peak for acetone ( $m = 58.0604$  a.m.u.) and the background  $(M-CH_3)^+$  ion of diethylamine ( $m = 58.0842$  a.m.u.) with ionization potentials of 9.7 and 7.8 eV, respectively. Moreover, peroxide radicals with different combinations of the number of atoms may have equal masses. In this situation, one must distinguish between ions with different atomic compositions but the same mass, i.e., there must be the possibility of analyzing mass spectra with high resolution.

The reader will recall that in the experiments we used mass spectrometers built in the Laboratory of Physical Electronics at the A F Ioffe Physico-Technical Institute of the Russian Academy of Sciences: a static sector magnetic mass spectrometer with a resolution  $R = 200$  [13], and a high-resolution magnetic resonance mass spectrometer with  $R = (2-3) \times 10^4$

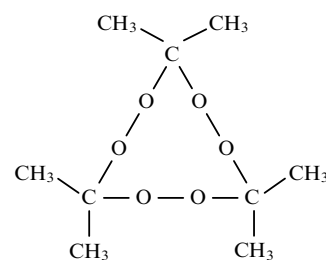


**Figure 12.** Structural formula of energy-saturated trimeric acetone peroxide (TAP) compound.

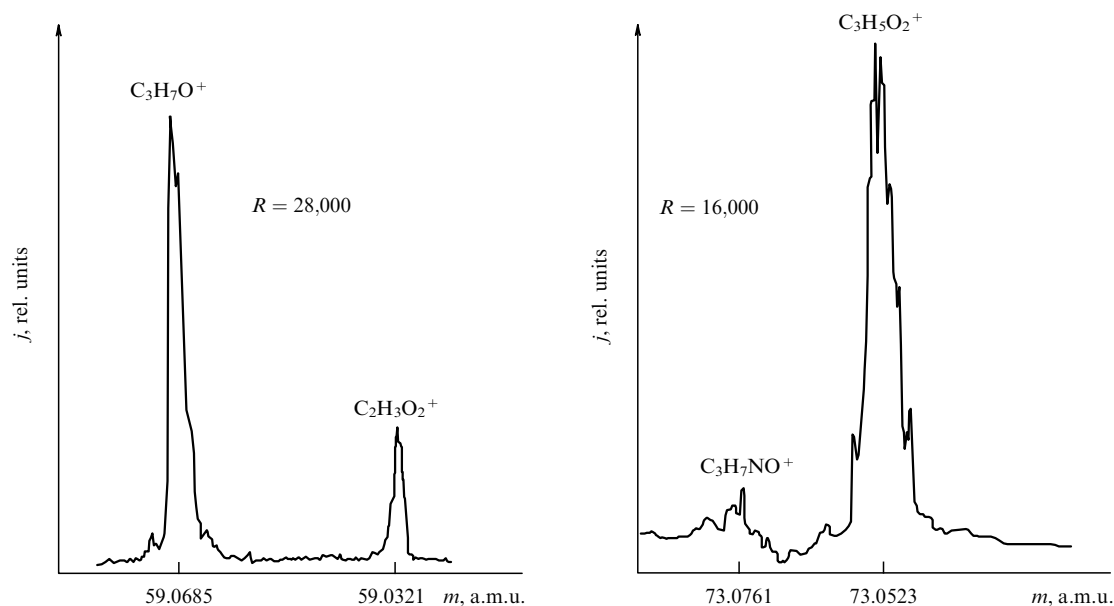


**Figure 13.** High-resolution mass spectra of surface ionization of TAP on oxidized tungsten at  $T = 1000$  K for  $m = 59$  a.m.u. and  $m = 73$  a.m.u.

[33], which were equipped with surface-ionization sources of ions and sources with ionization by electron impact. Tungsten ribbons and filaments served as emitters. With filaments we studied the effect of an electric field on TAP ionization. After heating the emitters at high temperatures, we oxidized them in an oxygen atmosphere.

The investigated ions of the peroxide radical with  $m = 73$  a.m.u. revealed in their high-resolution surface-ionization mass spectrum a small impurity peak (Fig. 13). The temperature of the distribution function of the main ion peak was found to be higher than the surface temperature by 500 K [31]. The peaks at  $m = 15$  a.m.u. and  $m = 89$  a.m.u. in the high-resolution surface-ionization mass spectrum were single and could be identified by the bench-mark method developed by us (see Ref. [33]). Ions with  $m = 15$  a.m.u. had the same temperature of the distribution function as the ions with  $m = 73$  a.m.u. [6]. Ions with  $m = 89$  a.m.u. were ionized at the surface in equilibrium conditions, i.e., the temperature of the distribution function was equal to the surface temperature (Fig. 14) [6]. High-resolution mass spectra guarantee that the temperature dependences belong not to two different ion peaks, as was the case with ions with  $m = 59$  a.m.u. (Fig. 13), but to the radicals  $\text{CH}_3$  with  $m = 15$  a.m.u.,  $(\text{CH}_3\text{O})\text{C}(\text{CH}_3)_2$  with  $m = 73$  a.m.u., and  $(\text{CH}_3\text{O})_2\text{CCH}_3$  with  $m = 89$  a.m.u.

The temperature dependences of the current of ions of the radical  $\text{CH}_3$  and other radicals, with the exception of the temperature curves in the cases with  $m = 73$  a.m.u. and  $m = 89$  a.m.u., were ascendant. For the  $\text{CH}_3^+$  ion, we found the experimental value  $\alpha_{\text{exp}} \sim 10^{-7} - 10^{-8}$  [6, 9] of the degree of surface ionization and the same quantity was calculated within the framework of the equilibrium theory [2]:  $\alpha_r = 10^{-13}$ . The ratio  $\alpha_{\text{exp}}/\alpha_r$  amounted to  $10^5 - 10^6$ , while the ratio  $\alpha_n/\alpha_r$  calculated by formula (12) for the ionization of the radical  $\text{CH}_3$  amounted to  $10^5 - 3 \times 10^5$ .

Comparison of all these values shows that although one cannot say that they coincide, they are close — by an order of magnitude. This confirms rather than refutes the assumption that such a significant increase in the surface ionization

effectiveness stems mainly from the vibrational excitation of adsorbed molecules, caused by the influx of energy liberated in the exothermic reaction of TAP disintegration at the surface. The smaller value of  $\alpha_n/\alpha_r$  is likely to be explained by the fact that the measured exponential temperature dependence of the  $\text{CH}_3^+$  ion current, which served as an

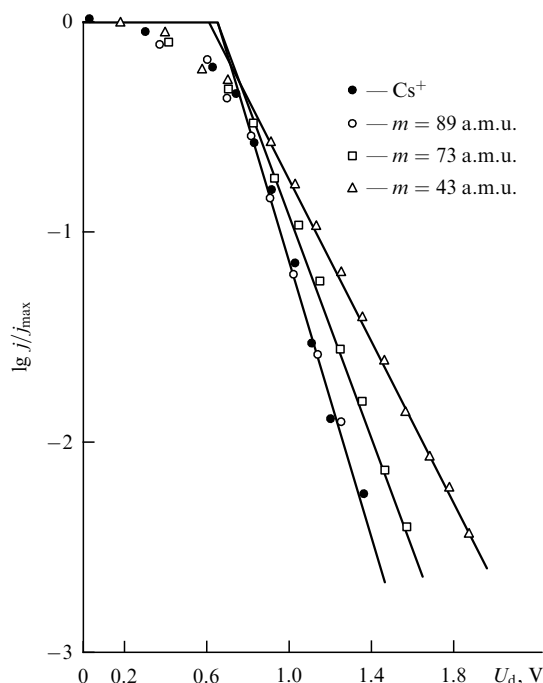


**Figure 14.** The delay curves  $\lg(j/j_{\text{max}})(U_d)$  for ions of fragments of TAP and ions of Cs atoms in surface ionization on oxidized tungsten at  $T = 1000$  K. The ion temperature  $T_d(\text{Cs}^+)$ , determined from the slope of the straight-line segment of the respective curve, coincides with the surface temperature. The temperature  $T_d(m = 73 \text{ a.m.u.})$  exceeds  $T_d(\text{Cs}^+)$  by 500 K, while the temperature  $T_d(m = 43 \text{ a.m.u.})$  exceeds  $T_d(\text{Cs}^+)$  by 800 K.

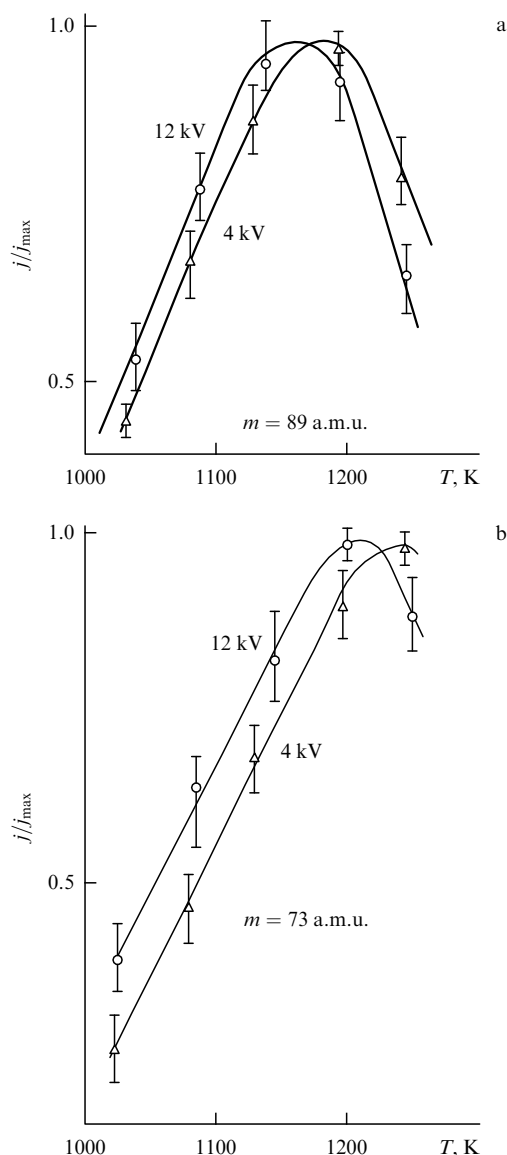


**Figure 15.** Temperature dependence  $(j/j_{\max})(T)$  of the current of ions of TAP fragments with masses  $m = 73$  a.m.u. and  $m = 89$  a.m.u. at  $F_1 = 1.1 \times 10^6$  V cm $^{-1}$  (4 kV) and  $F_2 = 3.4 \times 10^9$  V cm $^{-1}$  (12 kV) in the case of surface ionization on oxidized tungsten at  $T = 1000$  K.

argument in favor of using Eqn (12) in calculations, is actually the initial part of the bell-shaped temperature curve representing the disintegration of a multimolecular complex, a curve that does not fit the experimental temperature range whose use in calculations could produce a higher value of  $\alpha_n$ .

The temperature curves for the cases where  $m = 73$  a.m.u. and  $m = 89$  a.m.u. were bell-shaped (Fig. 15) and appeared shifted along the temperature axis to lower temperatures as the electric field strength increased, similar to the way the temperature curves for arduously ionizable substances behave [12]. This made it possible to measure the half-width of the temperature peaks for  $F = 3.4 \times 10^6$  V cm $^{-1}$ . In both cases, the measured half-width  $\delta T$  amounted approximately to 100–200 K.

When the half-width of the temperature curves of ion currents is small (see Section 2.5), the idea of a multimolecular complex is employed to describe the mechanism of formation of these ions.

In calculating the number of molecules in a multimolecular complex formed by molecules of trimeric acetone peroxide, one must bear in mind that the number of degrees of freedom of the complex calculated using the experimental data stems not from the sum of the degrees of freedom of the disintegration product considered (as it does, for instance, in the case of associative ions [18]) but from the sum of the degrees of freedom of the peroxide molecules ( $m = 222$  a.m.u. and  $s = 3n - 6 = 93$ ), whose ratio to the number of the degrees of freedom of the product considered ( $m = 73$  a.m.u. and  $s = 36$ ,  $m = 89$  a.m.u. and  $s = 39$ ) amounts, on the average, to roughly 2.5.

Here are data on a molecule of trimeric acetone peroxide and its disintegration products, which can be used to estimate the parameters of the multimolecular complex: for the TAP molecule  $(\text{CH}_3)_6(\text{O}_2)_3\text{C}_3$  —  $m = 222$  a.m.u., the number of atoms  $n = 33$ , and  $s = 93$ ; for the radical  $(\text{CH}_3\text{O})\text{C}(\text{CH}_3)_2$  —  $m = 73$  a.m.u.,  $n = 14$ ,  $s = 36$ ,  $b = 9-12$ , and  $\Delta T \sim 500$  K, and for the radical  $(\text{CH}_3\text{O})_2\text{CCH}_3$  —  $m = 89$  a.m.u.,  $n = 15$ ,  $s = 39$ ,  $b = 10-13$ , and  $\Delta T = 0$ .

The distribution function of ions of the radical with  $m = 89$  a.m.u. is close to the equilibrium one, with the result that to calculate the parameters of the radical of interest to us we can turn to Eqns (28) and (29). Thus, for the radical with  $m = 89$  a.m.u. we have  $b^* = 100$  and  $b^*k_B T_{\max} = 10$  eV.

If we assume that the average value of  $E_N$  is 0.7 eV [18], which can be found for a known ionization potential of associative ions, then for the ionization potential at  $m = 89$  a.m.u. we get  $eV \sim 8-9$  eV, which lands in the range of ionization potentials of oxygen-containing radicals. For a complex that would consist of the radicals with  $m = 89$  a.m.u., we would have  $N = 8$ , while for a complex consisting of peroxide molecules,  $N_{\text{TAP}} \sim 3$ .

To establish how  $\Delta T$  affects the parameters of the multimolecular complex, we calculated the temperature dependence of the ion current for the radical with  $m = 73$  a.m.u. at  $\Delta T = 500$  K and at  $\Delta T = 0$ .

At  $\Delta T = 0$ , Eqns (28) and (29) yield  $k_B T_{\max} b^* = 6.5$  eV and  $b^* = 61$ . Then using formula (28) one obtains  $eV \sim 5-6$  eV and  $N_{\text{TAP}} \sim 2$ . Here,  $V$  is much lower than the average values of the ionization potentials for such a class of substances. What is more, a radical with such an ionization potential is easily ionizable ( $e\varphi = 6.6$  eV), with the result that the ion current for the radical cannot depend on the electric field strength, which contradicts the results of the experiments.

Calculations that leaned upon Eqns (30) and (31) at  $\Delta T = 500$  K yielded  $k_B T_{\max} b_n^* = 19$  eV and  $b_n^* = 130$ . Then from Eqn (30) we get  $eV \sim 10-11$  eV and  $N_{\text{TAP}} \sim 3$ , which is in better agreement with the known data. The above values show that as the internal energy of the particles grows ( $\Delta T > 0$ ), an ever-increasing number of degrees of freedom of the particle participate in the dissociation process, which is quite natural.

The fact that the value  $N_{\text{TAP}}$  of the complex was obtained through an analysis of the temperature curves of the ion current for the radicals ionized in equilibrium and in nonequilibrium conditions makes this value more reliable and suggests that the phenomenologically derived (constructed) formula (19) for the ion current density of the radicals that are ionized by the nonequilibrium surface-ionization mechanism reflects, at least qualitatively, the complex processes of formation and disintegration of multimolecular complexes in nonequilibrium conditions. Our value of  $N_{\text{TAP}}$  also plays

an important role in explaining the results of experiments on intrinsic emission of optical radiation accompanying the heterogeneous decomposition of the peroxide in an electric field, which is the topic of Section 5.9.

### 5.9 Optical radiation and the ionization of hydrogen atoms under nonequilibrium surface ionization in an electric field

Experiments in which optical radiation emitted in the course of TAP disintegration in an electric field is detected and studied have been carried out at room temperature of an emitter being part of a surface-ionization field source of ions of an optical mass-spectrometry device [44]. For an emitter we used an oxidized tungsten filament 10  $\mu\text{m}$  in diameter, whose image was focused on the entrance slit of a MDR-23 optical spectrometer, which was part of a spectral computer complex KSVU-23. The TAP-vapor pressure amounted to roughly  $10^{-5}$  Torr, with the residual-gas partial pressures being at the level of  $10^{-8}$  Torr. All measurements were conducted in the 4000–7000-Å wavelength range. We detected five atomic emission lines, two of which belonged to the Na doublet, this element being an impurity in the material of the emitter. The three other emission lines were identified as the lines  $H_\alpha$ ,  $H_\beta$ , and  $H_\gamma$  of the Balmer series of the hydrogen atom (Fig. 16).

Studying the entire Balmer series requires exciting the hydrogen atom to an energy of 13.3 eV. The disintegration of a single acetone peroxide molecule is accompanied by the liberation of 135.4 kcal mol $^{-1}$  of energy ( $\sim 6.7$  eV), which is not enough to excite even lowest energy levels of H. On the other hand, the hydrogen atom can be excited if three peroxide molecules give out the energy, i.e., if a multimolecular complex disintegrates. However, the Balmer lines cannot be detected against the background if the electric field near the emitter is weak,  $F \sim (1-3) \times 10^5$  V cm $^{-1}$  (the ion-accelerating potential is in the 0.5–1-kV range). The lines appear only when the potential reaches the value of 7 kV, and their intensity increases by a factor of three to four as the potential grows to 13 kV ( $F \sim 4 \times 10^6$  V cm $^{-1}$ ).

A similar situation is observed for the  $H^+$  peak at an emitter temperature of 1000 K ( $m = 1$  a.m.u., with the ionization potential of the hydrogen atom being 13.6 eV), which appears when the accelerating potential is in the 6–7-kV range and increases by a factor of 10 to 15 as the potential grows to 15 kV. Since here there are no ion peaks corresponding to  $H_2O$  or OH radicals (with relatively low ionization potentials 12.6 and 13.2 eV, respectively), it is obvious that the hydrogen atom is ionized not by the field-evaporation mechanism but by the mechanism of surface ionization from an electronically excited state. However, the hydrogen atom in such excitation constitutes an easily ionizable element and its ion current should not increase with the field strength. We observed such independence from the field strength of the current of ions formed from electronically excited molecules in experiments in which we studied the surface ionization of anthracene molecules illuminated with the light from an ultraviolet (UV)  $N_2$ -laser whose lasing frequency coincided with the frequency of the first electronically excited level of the molecule [45].

A possible explanation of this effect of rising the intensity of emitted radiation for hydrogen atoms and their ion current with the electric field strength is that there is a shift in the equilibrium constant toward a more intense disintegration of the peroxide molecules (an increase in the reaction rate) due to the expulsion from the reaction of the disintegration products [10] through the ionic channel, since under such an increase in the field strength the ion currents rise by a factor of 100 to 1000.

Thus, the presence of radiation and of an ion current from hydrogen atoms in the heterogeneous disintegration of anthracene peroxide serves as indirect proof of the formation of multimolecular surface complexes from peroxide molecules.

The locations of the centers of the experimental peaks interpreted as  $H_\alpha$ ,  $H_\beta$ , and  $H_\gamma$  lines coincide, to within 2–5 Å, with the centers of the emission lines of a free hydrogen atom. The absence of shifts in the centers of the  $H_\alpha$ ,  $H_\beta$ , and  $H_\gamma$  lines suggests that the only hydrogen atoms that emit radiation are

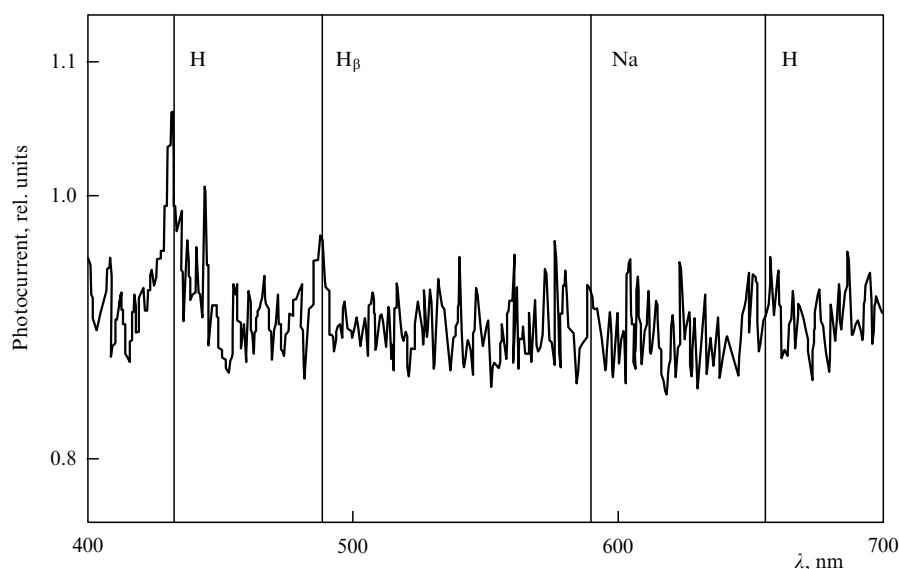


**Figure 16.** Emission spectrum recorded in the disintegration of TAP on the surface of oxidized tungsten at  $T = 300$  K with the electric field strength  $F$  at the emitter surface amounting to roughly  $4 \times 10^6$  V cm $^{-1}$ . The vertical straight lines mark the tabulated values of the Balmer series of the hydrogen atom ( $H_\alpha$ ,  $H_\beta$ , and  $H_\gamma$ ) and of the Na doublet (due to the large width of the monochromator slits, the Na doublet is not resolved).

those not incorporated into the molecular structures. The atoms of dissociated  $H_2$  molecules, residing at the surface in chemisorbed and physically adsorbed states, are, most probably, those that emit radiation. The center of a hydrogen atom in the state with  $n = 5$  has to be located at a distance of 12–13 Å from the surface, i.e., at a distance equal to the radius of the excited electron shell. Hydrogen atoms desorbing at an average rate that corresponds to the surface temperature ( $T = 300$  K) take about  $10^{-13}$  s (the lifetime of electronically excited states on oxidized tungsten [46]) to travel 4 Å. As a result, they find themselves in a situation where electron exchange with the surface of oxidized tungsten is highly improbable, since at larger distances the transparency of the barrier for electrons is low. The excited atoms are not ionized and continue to move away from the surface, emitting light in the course of their lifetime in the excited state. If for the sake of making an estimate we assume that the average lifetime is  $4 \times 10^{-8}$  s [46], the atoms travel, on the average, a distance of 60–70 μm, on which the electric field strength  $F \sim 3 \times 10^5$  V cm $^{-1}$ , which is lower than the quantum critical autoionization field strength  $F_0 \sim 10^6$  V cm $^{-1}$  for an excited hydrogen atom with  $n = 5$  [47].

Indeed, the results of calculations of the Stark broadening  $\Delta(H)$  of the lines  $H_\alpha$ ,  $H_\beta$ , and  $H_\gamma$  that allow, according to Condon and Shortley [48], for the effects of quadratic and cubic Stark effects in hydrogen show, when compared with the experimental data on the broadening of these lines (see Fig. 16), that the excited hydrogen atoms emit light in the electric fields of strength  $F \sim 3 \times 10^5$  V cm $^{-1}$  (Fig. 17).

Excited atoms that do not have enough thermal energy to be desorbed are ionized by the surface-ionization mechanisms, just as easily ionizable substances are.

What makes the intrinsic emission of radiation by the adsorbed atoms in heterogeneous TAP disintegration so

unusual is that the formation of electronically excited particles of the second and (even more so) third generations in the gas phase is highly improbable [7], i.e., a unique property of surfaces — to be conducive to the interaction of components on the surface — manifests itself here.

The discovered phenomenon of the emission of radiation of the Balmer series by adsorbed hydrogen atoms has an interesting astrophysical consequence. In the process of formation of molecules from free atoms in cosmic gas–dust clouds, on the surface of dust particle there appears an atomic–molecular condensate with high internal energy (accumulated in cryogenic adsorption) [49], which in the process of disintegrating transfers its energy to the adsorbed hydrogen atoms. Hence, the emission of hydrogen lines observed by astrophysicists may, at least theoretically, be caused by the emission of radiation from the surface of dust particles and not only by the interstellar gas medium in the line of sight.

### 5.10 Nonequilibrium surface ionization with external excitation of the vibrational states of the adsorbate (photodesorption field IR spectroscopy)

The adequacy of the description of the exponential increase in ion emission from a vibrationally excited state of the adsorbate has made it possible to assume that the absorption of radiation by adsorbed molecules within the range of their intrinsic vibrational bands would lead to an increase in ion emission by the mechanism of nonequilibrium surface ionization. Experiments in this area of research formed a basis for developing a new method called the photodesorption field IR spectroscopy [43].

The reader will recall that the proposed method establishes a relation between the current of ions being desorbed from a surface (in the presence of a strong electric field) and the varying frequency of IR radiation, which corresponds to the natural vibrations of the adsorbed molecules, impinging on that surface. Thus, the recorded spectrum (i.e., the dependence of the ion current on the radiation frequency) makes up the desorption vibrational spectrum of adsorbed molecules and their fragments.

The ion emitter was an oxidized tungsten filament 5 μm in diameter. The electric field strength near the emitter could be varied from  $10^5$  to  $8 \times 10^6$  V cm $^{-1}$  in the smooth-filament mode, and up to  $10^8$  V cm $^{-1}$  in the tungsten-oxide scales growing mode [50]. The residual gas pressure in the chamber amounted to  $10^{-9}$  Torr, and the pressure of the water vapor, whose desorption spectrum was being investigated, was set at a  $(1-2) \times 10^{-6}$  Torr. In the experiments, the emitter temperature amounted to 350–400 K. The recording (scanning) of the spectrum was done with a sweep along the (horizontal) wavelength axis within two ranges, viz. 1600–2000 nm and 2000–3000 nm, with a 20-nm increment. In each spectrum range, a background scan (without illuminating the emitter) was taken, which was followed by a scan with the emitter being illuminated. The difference between the second and first scans was considered the working scan. The statistics in each range consisted of 110 and 80 working scans, respectively.

Figure 18 shows two spectra: with 66 working scans (Fig. 18a) [51] and with 110 working scans (Fig. 18b) [44], of the ion current for  $H_2O^+$  ( $m = 18$  a.m.u.) with a sweep of the radiation in wavelengths in the 1.6–2-μm range. The excess of the current over the root-mean-square deviation of the values of the background current was observed at  $\lambda = 1.91$ –

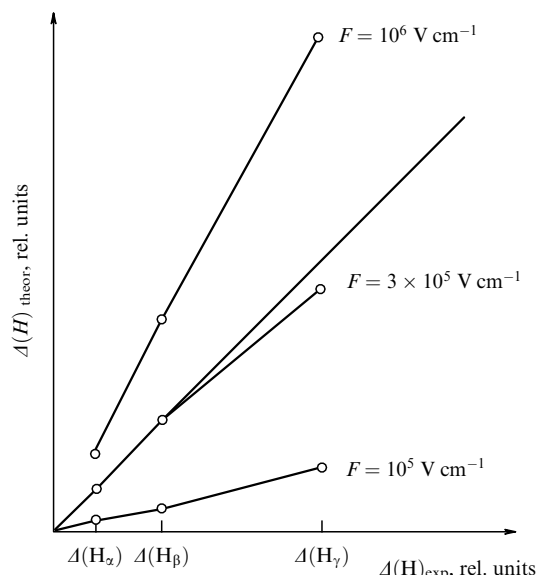


**Figure 17.** Comparison of experimental and theoretical values of the broadening ( $\Delta$ ) of the lines belonging to the Balmer series of the hydrogen atom,  $\Delta(H_\alpha)$ ,  $\Delta(H_\beta)$ , and  $\Delta(H_\gamma)$ , in electric fields. The experimental values are marked off on the horizontal axis, while the theoretical broadening values corresponding to the experimental values  $\Delta(H_\alpha)$ ,  $\Delta(H_\beta)$ , and  $\Delta(H_\gamma)$  are marked off on the vertical axis for different values of the field strength  $F_i$ . Points near the straight line that passes through the origin at an angle of 45° correspond to a field for which the experimental and theoretical values coincide.

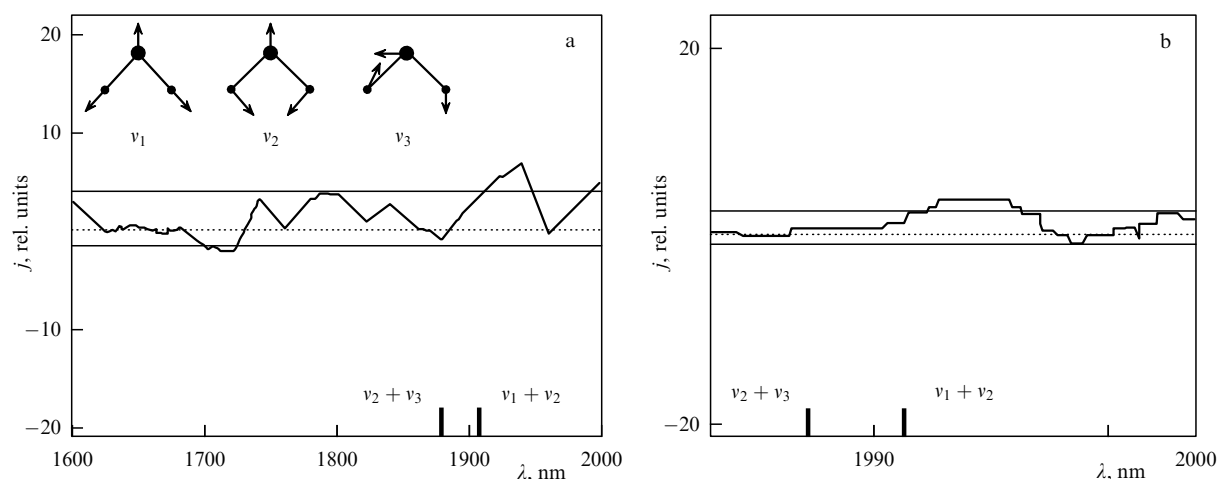


**Figure 18.** Spectral dependences of the current,  $j(\lambda)$ , of  $\text{H}_2\text{O}^+$  ions being desorbed in a strong electric field ( $F \sim 10^8 \text{ V cm}^{-1}$ ) when near-IR radiation irradiates water molecules adsorbed on oxidized tungsten at  $T = 350 \text{ K}$ : (a) the statistics of 66 scans, and (b) the statistics of 110 scans. The scales of the vertical axes in (a) and (b) figures are the same. The horizontal straight lines indicate the root-mean-square error.

$1.95 \mu\text{m}$ . The closest to these wavelengths are the composite wavelengths corresponding to the natural frequencies of water molecules:  $(\nu_1 + \nu_2)^{-1} = 1.91 \mu\text{m}$ , and  $(\nu_2 + \nu_3)^{-1} = 1.88 \mu\text{m}$ . Here, we employed the common notation for normal parallel vibrations: the skeleton  $(\nu_1)^{-1} = 2.73 \mu\text{m}$  and the deformation  $(\nu_2)^{-1} = 6.27 \mu\text{m}$ , and for the perpendicular skeleton vibration  $(\nu_3)^{-1} = 2.66 \mu\text{m}$  [52].

Vibrations with the composite frequency  $\nu_2 + \nu_3$ , as well as those with the fundamental frequency  $\nu_3$ , are not excited on the surface if the symmetry axis of an adsorbed water molecule is perpendicular to the surface (such an arrangement of water molecules, especially in an electric field, is the most probable one). The dipoles that are parallel to the surface are not excited, since the respective component in the radiation field incident on the metal surface is zero [43]. Thus, the observed band can be considered belonging to vibrations with the composite frequency  $\nu_1 + \nu_2$ . The width of this band in the desorption spectrum is roughly  $100 \text{ cm}^{-1}$ , which corresponds to the width of the band for a separate molecule. This means that the adsorbed molecules are not linked by hydrogen bonds, i.e., do not form a water film on the surface [53]. The shift in the absorption band by  $130 \text{ cm}^{-1}$  suggests the presence of a chemical shift that overlaps the dipole interaction of the adsorbed molecules [43].

A few words about the possible manifestation of the band of skeleton vibrations  $\nu_1$ . Analysis of the spectra in the  $2 - 3\text{-}\mu\text{m}$  range revealed no statistically significant ion-current bursts. Nevertheless, a change in the shape of a noise track was recorded, in particular, a decrease in the number of passages of the noise line through zero by a factor of two to three in the vicinity of  $\lambda = 2.7 \mu\text{m}$ .

Bearing in mind that the intensity of the band corresponding to the frequency  $\nu_1$  is lower than that of the band corresponding to  $\nu_2$  [52], we can conclude that the probability of water molecule desorption from the surface is highest for the molecules performing deformation vibrations. We can also assume that water molecules are adsorbed on the surface by oxygen atoms. The latter assumption follows from the fact that the frequencies of the deformation vibrations of adsorbed and free molecules are almost the same: these frequencies are determined by the movement of hydrogen atoms toward each other, and these movements

remain free as oxygen atoms adsorb water molecules. The absence of absorption bands with perpendicular vibrations  $\nu_3$  suggests that the symmetry axis of water molecules is perpendicular to the surface.

### 5.11 Absorption cross section of IR radiation by adsorbed molecules

Unfortunately, not all of the experimentally examined quantities in formula (42) were determined in our experiments. For instance, we were unable to measure  $\Delta T$  by the delay method due to the small values of the current  $\Delta j$ .

The ionization potential for water molecules was taken from tables:  $eV = 12.6 \text{ eV}$ . The value of the equilibrium current  $j$  was used to estimate the field strength close to  $F \sim 10^8 \text{ V cm}^{-1}$ . The value of  $e\phi$ , determined from the temperature curves for bismuth ions, amounted to  $6.7 \pm 0.05 \text{ eV}$ . The intensity of radiation equal to  $I \sim 10^{18}$  photons per  $1 \text{ cm}^2$  per second was estimated on the grounds of the electric power of the emitter, its temperature corrected for blackbody radiation, and with allowance for the aperture ratio of the monochromator. The value of  $\tau_i$  can be estimated bearing in mind the following: the experimentally established fact that the distribution of excited ions over the velocities of translational motion approaches the Maxwellian distribution suggests that the ionization of excited molecules has to do with adiabatic transitions rather than with vertical transitions. In other words, after absorption of IR photons and subsequent ionization, there is still time for stochastization of the energy absorbed by a particle among its degrees of freedom, including the translational degrees of freedom. For this to materialize, the ions must have time to perform at least a few vibrations, i.e.,  $\tau_i$  cannot be shorter than  $10^{-12} - 10^{-13} \text{ s}$ .

For the value of  $\Delta j$  we took the excess of the current over the root-mean-square deviation from the average current value in the working scan. Hence, it was assumed that, on the whole, the spread of  $j$  values corresponds to a normal distribution, while the deviation of the current from this distribution is determined, at a confidence level of about 0.67, by a systematic factor: in our case, the vibrational excitation of ions. The magnitude of the exponent in formula (42) was estimated to lie within the limits of variation of  $\Delta T \sim 10 - 50 \text{ K}$ . Under these assumptions and with the

experimental value of the ratio  $\Delta j/j \sim 10^{-3}$ , the magnitude of the cross section of the process, calculated according to Eqn (42), was found to vary within the range from  $10^{-11}$  to  $10^{-12}$  cm<sup>2</sup>. Such high magnitudes of the cross section  $\sigma$ , compared to the respective values for the gas phase, for different processes involving adsorbed molecules have been evidenced in several experiments (see Refs [54, 55]), but have yet to be explained theoretically.

### 5.12 Ratio of partition functions of the neutral and ionic states in a polyatomic molecule

In this section we describe a procedure of measuring the ratio of the partition functions of the neutral and ionic states in polyatomic molecules [56]. Knowing these partition functions is interesting as a separate aspect, but since there is practically no way in which they can be evaluated theoretically, their ratio was assumed *a priori* to be equal to unity [4].

The experiments involved studying the field surface ionization of anthracene, which forms a molecular ion, and of bismuth in electric fields with strengths ranging from  $9 \times 10^5$  to  $4.5 \times 10^6$  V cm<sup>-1</sup>. The dependence of the current density  $j(T, F)$  of molecular ions in the initial sections of the temperature curves and of atomic ions is described by the following classical expression [2]:

$$j = \frac{eg}{1 + (Q^0/Q^+) \exp \left\{ [e(V - \varphi - \sqrt{eF})]/k_B T \right\}}. \quad (43)$$

The total partition functions for polyatomic particles can be represented in the form of products of the partition functions in each type of motion [57]:  $Q = Q_{tr} Q_{rot} Q_{vib} Q_{el}$ , where  $Q_{tr}$ ,  $Q_{rot}$ ,  $Q_{vib}$ , and  $Q_{el}$  are the partition functions of the translational, rotational, vibrational, and electronic states of the particle, respectively. The ratio of the partition functions of the neutral and ionic states in polyatomic particles can be written down as follows:

$$\frac{Q^0}{Q^+} = \frac{Q_{vib}^0 Q_{el}^0}{Q_{vib}^+ Q_{el}^+}. \quad (44)$$

The ratio  $Q_{tr}^0/Q_{tr}^+$  is assumed equal to unity, since the masses of the ion and the neutral particle are practically the same, and, since ionization has practically no effect on the conformation of the anthracene molecule, the ratio  $Q_{rot}^0/Q_{rot}^+$  is also equal to unity. By studying the function  $j(F)$  for known values of  $V$  and  $\varphi$  with  $F = \text{const}$  and  $T = \text{const}$  we can determine the ratio  $Q^0/Q^+$ .

The emitter in the experiments was an oxidized tungsten filament 10  $\mu\text{m}$  in diameter. The emitter temperature was kept at  $1100 \pm 20$  K. The pressure of anthracene vapor was  $2 \times 10^{-7}$  Torr. The work function of the emitter, determined from the temperature dependence of the current of bismuth ions at minimum electric field strength, amounted to  $6.57 \pm 0.05$  eV. Figure 19 illustrates the dependences of the currents of bismuth ions (the points in curve 1) and of anthracene ions (the points in curve 2) on the electric field strength. The solid curve 1 represents the results of numerical calculations by formula (43) for bismuth with the following parameters:  $T = 1100$  K,  $e\varphi = 6.6$  eV, and  $eV = 7.286$  eV.

The partition-function ratio  $Q^0/Q^+$  for bismuth was assumed equal to four, since the ground state of bismuth atoms is  $^4S_{3/2}$  [58] (orbital quantum number  $L = 0$ , total spin  $S = 3/2$ , and total angular momentum  $J = 3/2$ ). Since  $L = 0$ , there is no fine splitting, but the level is degenerate in the

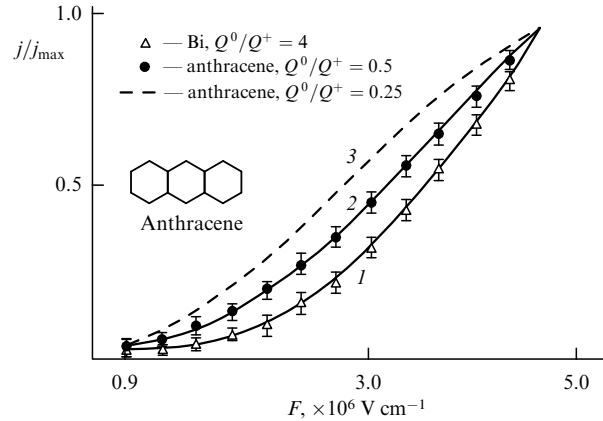


**Figure 19.** Field curves of the relative currents  $(j/j_{\max})(F)$  of bismuth ions and of anthracene molecular ions  $(C_{14}H_{10})^+$  in surface ionization on oxidized tungsten at  $T = 1100$  K. The dashed curve represents the results of theoretical calculations under the assumption that the ratio  $Q^0/Q^+$  of the partition functions of the neutral and ionic states in anthracene is 0.25.

direction of the total angular momentum  $J$ . The degree of degeneracy  $2J + 1$  is equal to four, with the result that the multiplicity of the ground state in the bismuth atom is also equal to four. The transition energy to the first excited state amounts to 4 eV, so that the probability of its thermal excitation is practically zero. The multiplicity of the bismuth ion is equal to unity, since the ground state of the ion is  $^3P_0$  ( $L = 1$ ,  $S = 1$ , and  $J = 0$ ). In the case at hand there is level fine splitting, whose multiplicity is equal to three (either  $2L + 1$  or  $2S + 1$ ).

Thus, there emerge three levels that differ in values of the total angular momentum  $J$ : levels with  $J = 2, 1, 0$ . In the ground state of the ion, one has  $J = 0$ , and the energy of excitation from this state to the nearest state ( $J = 1$ ) amounts to 1.65 eV [58]. The probability of such a population of the excited state at 1100 K is around  $10^{-7}$ , so that we can ignore it in the partition function. Since  $J = 0$ , there is no degeneracy in the direction of the total angular momentum, with the result that the partition-function ratio for bismuth is  $Q^0/Q^+ = 4$ .

Figure 19 clearly shows that there is good agreement between the theoretical curve and the experimental results. Notice that for the theoretical curve to fit better the experimental points the work function was varied within the limits of errors in measuring  $\varphi$  at a fixed value of  $Q^0/Q^+$ . The result was  $e\varphi = 6.60 \pm 0.2$  eV. Curve 2 represents the results of a numerical calculation of the anthracene ion current with the following values of the parameters:  $T = 1100$  K,  $eV = 7.38$  eV [59], and  $e\varphi = 6.60$  eV. The partition-function ratio was varied in order to obtain the best fit of the theoretical curve to the experimental points. The best result achieved was  $Q^0/Q^+ = 0.50 \pm 0.04$ . Curve 3, calculated for anthracene with a partition-function ratio of  $1/4$ , shows the sensitivity of this method to determining the ratio. Ratio (44) consists of two factors: the ratio of the partition functions of the electronic states, and the ratio of the statistical functions of the vibrational states of the neutral particle and the ion.

Peacock and Wilkinson [60] showed that all the orbitals of the anthracene molecule are completely filled and that the multiplicity of the ground state is equal to unity. They also found that there are two electrons on the upper orbital of the



anthracene molecule, so that removal of one such electron results in an ionic state with the spin  $S = 1/2$  and multiplicity  $2S + 1 = 2$ , and since the law of conservation of orbital momentum does not work in polyatomic molecules, the multiplicity of the ionic state is determined solely by spin multiplicity, with the result that  $Q^0/Q^+ = 1/2$ , which coincides with the experimental result. As for the vibrational spectrum, Hiraya [61] found for the ion of naphthalene (a homolog of anthracene) that the vibrational frequencies of the ion are lower than those for the neutral molecule. We estimated the ratio of the vibrational partition functions of the molecule and ion of naphthalene on the basis of Hiraya's data and found it to be close to unity (0.85). Since  $Q^0/Q^+$  for anthracene is equal to  $1/2$ , we may conclude that in this case the vibrational spectra of the ion and the neutral molecule coincide.

This result suggests that for radicals the ratio of the partition functions of neutral particles and ions must be close to two if their vibrational partition functions are the same, as they are in the case of anthracene, since radicals have an unpaired electron, i.e., the multiplicity of the electronic state of a radical is equal to two, and that of its ion to unity.

## 6. Conclusions

In addition to the concept of surface ionization, we introduced the idea of nonequilibrium surface ionization. Within the scope of this idea, we examined the desorption of polyatomic ions from vibrationally excited and vibrationally deactivated states with respect to the states determined by the surface temperature. To describe the process quantitatively, we carried out a statistical derivation of the degree of nonequilibrium surface ionization. The resulting analytical expressions for the dependences of the ion flux on the electric field strength, the temperature of the energy distribution function, and the surface temperature make it possible to calculate the ion currents of the products of exothermic and endothermic heterogeneous disintegration reactions. The calculated values of the ion currents are in satisfactory agreement with the experimental results.

It has been predicted (as a consequence of the theory of nonequilibrium surface ionization in an electric field) and corroborated in experiments that the current of the ions of adsorbed molecules rises in the event of resonant absorption of IR radiation by these molecules in the range of the frequencies of the natural vibrations of the molecules. The experimental data were used to determine the type of vibrations responsible for desorption of water ions from a surface. On the basis of the expression for the degree of nonequilibrium surface ionization, we estimated the magnitude of the cross section of IR radiation absorption by the adsorbed molecules.

By comparing, within the framework of the theory of surface ionization, the results of an analysis of the kinetics of monomolecular reactions on a surface, the results of statistical theories, and experimental data we concluded that the processes of monomolecular disintegration on a surface are of the nonequilibrium character. Using the resulting analytical expressions for surface ionization with nonequilibrium distribution functions, we were able to numerically determine the following parameters of the heterogeneous reactions: (a) the dissociation activation energy of molecules on a surface; (b) the number of effective degrees of freedom of molecules on the surface; (c) the ionization potentials of

radicals; (d) the time it takes the surface and the products of monomolecular disintegration reactions to exchange energy, and (e) the magnitude of reaction departure from equilibrium, which is the difference between the temperature of the distribution function of ions produced in the first stages of the reaction and the surface temperature.

As a result of an analysis of the potential curves, we established the presence of a polarization interaction between polyatomic ions and a metal surface and the flow of charge between like atoms of polyatomic ions along the electric lines of force. We also found the potential curves for the polarization interaction between polyatomic ions.

We examined the mechanism of formation, at relatively low temperatures of the emitter, of narrow bell-shaped curves representing the dependence of the flux of molecules and ions being desorbed from the surface on the surface temperature. We also developed a model that makes it possible, in the cases of surface ionization and nonequilibrium surface ionization, to examine, from a single viewpoint, the processes of formation of multimolecular complexes on a surface and their disintegration into fragments by the mechanism of monomolecular reactions, with subsequent ionization of these fragments at the surface. The resulting analytical expressions of this model (for the field and temperature dependences of the ion current) allowed us to estimate, on the grounds of experimental data, the number of molecules in a complex, the ionization potentials of the fragments, and the number of effective degrees of freedom of the complex.

We found that the measured ratio of the total partition functions of the neutral and ionic states in a polyatomic molecule (anthracene) is determined by its spin multiplicity.

We also discovered the existence of a physically adsorbed state of polyatomic ions in an electric field accelerating ions.

This article generalizes for the first time results in surface ionization with nonequilibrium distribution functions and in the nonequilibrium surface ionization of fragments of polyatomic molecules that form as a result of reactions at the surface and proposes methods for studying and analyzing the experimental results obtained by an entirely new method — surface-ionization field mass spectrometry.

The authors would like to express profound gratitude to A A Kaplyanskii and N D Potekhina, who took the trouble to read the manuscript of this article and made useful suggestions and remarks.

Partial support of this work was provided by the Russian Foundation for Basic Research (grant Nos 01-02-17803 and 04-02-17658).

## References

1. Zandberg É Ya, Ionov N I *Usp. Fiz. Nauk* **67** 581 (1959) [*Sov. Phys. Usp.* **2** 255 (1959)]
2. Zandberg E Ya, Ionov N I *Poverkhnostnaya Ionizatsiya* (Surface Ionization) (Moscow: Nauka, 1969); see also Ionov N I *Surface Ionization and Its Applications* (Oxford: Pergamon Press, 1972)
3. Zandberg E Ya, Rasulev U Kh, Shustrov B N *Dokl. Akad. Nauk SSSR* **172** 885 (1968)
4. Zandberg E Ya, Rasulev U Kh *Usp. Khim.* **51** 1425 (1982) [*Russ. Chem. Rev.* **51** 819 (1982)]
5. Potekhina N D *Teor. Eksp. Khim.* **9** 606 (1973) [*Theor. Exp. Chem.* **9** 476 (1973)]
6. Bakulina I N et al. *Pis'ma Zh. Tekh. Fiz.* **1** 170 (1975) [*Sov. Tech. Phys. Lett.* **1** 81 (1975)]

7. Kondrat'ev V N, Nikitin E E *Kinetika i Mekhanizm Gazofaznykh Reaktsii* (Gas-Phase Reactions: Kinetics and Mechanisms) (Moscow: Nauka, 1975) [Translated into English (Berlin: Springer-Verlag, 1981)]
8. Shelepin L A *Vdali ot Ravnovesiya* (Far from Equilibrium) (New Ideas in Life, Science, and Technology: Physics Series, No. 8) (Moscow: Znanie, 1987)
9. Lavrent'ev G Ya, Thesis for Doctorate of Physicomathematical Sciences (St.-Petersburg: A F Ioffe Physico-Technical Institute of the Russian Academy of Sciences, 2003)
10. Panchenkov G M, Lebedev V P *Khimicheskaya Kinetika i Kataliz* (Chemical Kinetics and Catalysis) 3rd ed. (Moscow: Khimiya, 1985) [Translated into English (Moscow: Mir Publ., 1976)]
11. Lavrent'ev G Ya *Pis'ma Zh. Tekh. Fiz.* **27** (10) 52 (2001) [*Tech. Phys. Lett.* **27** 419 (2001)]
12. Blashenkov N M, Ionov N I, Lavrent'ev G Ya *Pis'ma Zh. Tekh. Fiz.* **13** 392 (1987) [*Sov. Tekh. Phys. Lett.* **13** 160 (1987)]
13. Blashenkov N M, Ionov N I, Lavrent'ev G Ya *Teor. Eksp. Khim.* **24** 62 (1988) [*Theor. Exp. Chem.* **24** 57 (1988)]
14. Korol' E N et al. *Fizicheskie Osnovy Polevoi Mass-Spektrometrii* (Physical Foundations of Field Mass Spectrometry) (Gen. Ed. E N Korol') (Kiev: Naukova Dumka, 1978)
15. Ionov N I, Mittsev M A *Zh. Tekh. Fiz.* **35** 1863 (1965) [*Sov. Tech. Phys.* **10** 1436 (1966)]
16. Lavrent'ev G Ya *Zh. Tekh. Fiz.* **71** (10) 120 (2001) [*Tech. Phys.* **46** 1322 (2001)]
17. Tsong T T *Surf. Sci. Rep.* **8** 127 (1988)
18. Blashenkov N M, Lavrent'ev G Ya *Pis'ma Zh. Tekh. Fiz.* **31** (16) 1 (2005) [*Tech. Phys. Lett.* **31** 629 (2005)]
19. Blashenkov N M, Lavrent'ev G Ya *Pis'ma Zh. Tekh. Fiz.* **14** 1359 (1988) [*Sov. Tech. Phys. Lett.* **14** 593 (1988)]
20. Dobretsov L N, Gomoyunova M V *Emissionnaya Elektronika* (Emission Electronics) (Moscow: Nauka, 1966) [Translated into English (Jerusalem: Israel Program for Scientific Translation, 1971)]
21. Blashenkov N M, Lavrent'ev G Ya *Pis'ma Zh. Tekh. Fiz.* **25** (14) 42 (1999) [*Tech. Phys. Lett.* **25** 505 (1999)]
22. Blashenkov N M, Lavrent'ev G Ya *Zh. Tekh. Fiz.* **61** (1) 155 (1991) [*Sov. Tech. Phys.* **36** 93 (1991)]; Blashenkov N, Lavrent'ev G, in *IV Nordic Conf. of Surface Science, Norway, 1997*, p. 161
23. Blashenkov N M, Lavrent'ev G Ya *Pis'ma Zh. Tekh. Fiz.* **21** (24) 15 (1995) [*Tech. Phys. Lett.* **21** 1000 (1995)]
24. Kel'man V M, Yavor S Ya *Elektronnaya Optika* (Electron Optics) 3rd ed. (Leningrad: Nauka, 1968)
25. Bakulina I N et al., Author's Certificate No. 711935 (1987); *Byull. Izobret.* (48) (1987)
26. Simpson J A *Rev. Sci. Instrum.* **32** 1283 (1961) [*Prib. Nauch. Issled.* (12) 3 (1961)]
27. Blashenkov N M, Lavrent'ev G Ya *Zh. Tekh. Fiz.* **54** 2274 (1984)
28. Blashenkov N M, Lavrent'ev G Ya *Zh. Tekh. Fiz.* **54** 410 (1984)
29. Blashenkov N M, Lavrent'ev G Ya *Pis'ma Zh. Tekh. Fiz.* **22** (7) 1 (1996) [*Tech. Phys. Lett.* **22** 293 (1996)]; also in *Prog. and Abstr. 43rd Intern. Field Emission Symp., Moscow, July 14–19, 1996*, p. 76
30. Zandberg E Ya, Nazarov E G, Rasulev U Kh *Zh. Tekh. Fiz.* **50** 1752 (1980)
31. Paleev V I *Teor. Eksp. Khim.* **19** 214 (1983) [*Theor. Exp. Chem.* **19** 192 (1983)]
32. Rasulev U Kh, Thesis for Doctorate of Physicomathematical Sciences (Leningrad: A F Ioffe Physico-Technical Institute of the USSR Academy of Sciences, 1979)
33. Blashenkov N M, Lavrent'ev G Ya, Shustrov B N *Zh. Tekh. Fiz.* **58** 1609 (1988) [*Sov. Tech. Phys.* **33** 973 (1988)]
34. Zandberg E Ya, Ionov N I *Zh. Tekh. Fiz.* **28** 2445 (1958)
35. Schottky W *Ann. Phys. (Leipzig)* **62** 143 (1920)
36. Woodruff D P, Delchar T A *Modern Techniques of Surface Science* (Cambridge: Cambridge Univ. Press, 1986) [Translated into Russian (Moscow: Mir, 1989)]
37. Letokhov V S *Lazernaya Fotoionizatsionnaya Spektroskopiya* (Laser Photoionization Spectroscopy) (Moscow: Nauka, 1987) [Translated into English (Orlando: Academic Press, 1987)]
38. Zandberg E Ya, Rasulev U Kh *Teor. Eksp. Khim.* **7** 363 (1971) [*Theor. Exp. Chem.* **7** 299 (1973)]
39. Blashenkov N M, Lavrent'ev G Ya *Zh. Tekh. Fiz.* **60** (2) 154 (1990) [*Sov. Tekh. Phys.* **35** 227 (1990)]
40. Zandberg E Ya, Nazarov E G, Rasulev U Kh, in *Mass-Spektrometriya i Khimicheskaya Kinetika* (Mass Spectrometry and Chemical Kinetics) (Ed.-in-Chief V L Tal'roze) (Moscow: Nauka, 1985) p. 192
41. Hudson D J "Statistics: Lectures on Elementary Statistics and Probability", CERN Report 63–29 (Geneva: CERN, 1964) [Translated into Russian (Moscow: Mir, 1970)]
42. Hirschfelder J O, Curtiss C F, Bird R B *The Molecular Theory of Gases and Liquids* (New York: Wiley, 1954) [Translated into Russian (Moscow: IL, 1961)]
43. Willis R F, in *Vibrational Spectroscopy of Adsorbates* (Springer Ser. in Chem. Phys., Vol. 15, Ed. R F Willis) (Berlin: Springer-Verlag, 1980) [Translated into Russian (Moscow: Mir, 1984) p. 11]
44. Blashenkov N M, Lavrent'ev G Ya *Zh. Tekh. Fiz.* **69** (9) 123 (1999) [*Tech. Phys.* **44** 1111 (1999)]; also in *Prog. and Abstracts 45 Intern. Field Emission Symp., Jordan, September 1998*, p. 120
45. Blashenkov N M, Lavrent'ev G Ya, in *Tezisy Dokl. XXII Konf. po Emissionnoi Elektronike* (Abstr. 22nd Conf. on Emission Electronics) Vol. 2 (Tashkent: FAN, 1994) p. 112
46. Ageev V N, Yakshinskii B V *Fiz. Tverd. Tela* **27** 99 (1985) [*Sov. Phys. Solid State* **27** 57 (1985)]
47. Bethe H A, Salpeter E E *Quantum Mechanics of One- and Two-Electron Atoms* (Berlin: Springer-Verlag, 1957) [Translated into Russian (Moscow: Fizmatgiz, 1960)]
48. Condon E U, Shortley G H *The Theory of Atomic Spectra* (Cambridge: The Univ. Press, 1944) [Translated into Russian (Moscow: IL, 1949)]
49. Bakulina I N et al. *Astron. Zh.* **57** 352 (1980) [*Sov. Astron.* **24** 203 (1980)]; Lavrent'ev G Ya, Thesis for Candidate of Physicomathematical Sciences (Leningrad: A F Ioffe Physico-Technical Institute of the USSR Academy of Sciences of USSR, 1988)
50. Beckey H D *Principles of Field Ionization and Field Desorption Mass Spectrometry* (Intern. Ser. in Analytical Chemistry, Vol. 61) (Oxford: Pergamon Press, 1977)
51. Blashenkov N M, Lavrent'ev G Ya *Pis'ma Zh. Tekh. Phys.* **23** (23) 22 (1997) [*Tekh. Phys. Lett.* **23** 909 (1997)]
52. Gribov L A *Vvedenie v Molekulyarnuyu Spektroskopiya* (Introduction to Molecular Spectroscopy) (Moscow: Nauka, 1976)
53. Bobovich Ya S *Usp. Fiz. Nauk* **162** (6) 81 (1992) [*Sov. Phys. Usp.* **35** 481 (1992)]
54. Zandberg E Ya et al. *Izv. Akad. Nauk SSSR, Ser. Fiz.* **56** (8) 21 (1992) [*Bull. Acad. Sci. USSR, Ser. Phys.* **56** 1136 (1992)]
55. Dixon-Warren St J et al. *J. Chem. Phys.* **88** 4092 (1988)
56. Blashenkov N M, Lavrent'ev G Ya *Pis'ma Zh. Tekh. Fiz.* **16** (4) 72 (1990) [*Sov. Tech. Phys. Lett.* **16** 154 (1990)]
57. Levich V G *Kurs Teoreticheskoi Fiziki* (Course in Theoretical Physics) 2nd ed. (Moscow: Nauka, 1969) [Translated into English: *Theoretical Physics: an Advanced Text* (Amsterdam: North-Holland, 1970–1973)]
58. Radzig A A, Smirnov B M *Parametry Atomov i Atomnykh Ionov* (Parameters of Neutral Atoms and Atomic Ions) 2nd ed. (Moscow: Energoatomizdat, 1986) [Translated into English as *Reference Data on Atoms, Molecules, and Ions* (Berlin: Springer-Verlag, 1985)]
59. Kondrat'ev V N (Exec. Ed.) *Energii Razryva Khimicheskikh Svyazei. Potentsialy Ionizatsii i Srodstvo k Elektronu* (Chemical Bond Rupture Energies. Ionization Potentials and Electron Affinity) (Moscow: Nauka, 1974)
60. Peacock T E, Wilkinson P T *Proc. Phys. Soc. London* **83** 525 (1964)
61. Hiraya A *J. Chem. Phys.* **82** 1810 (1985)